Recent Developments of Surface Parameterization Methods Using Quasi-conformal Geometry

43

Gary P. T. Choi and Lok Ming Lui

Contents

G. P. T. Choi
Department of Mathematics, Massachusetts Institute of Technology, Cambridge, MA, USA
e-mail: ptchoi@mit.edu

L. M. Lui (✉)
Department of Mathematics, The Chinese University of Hong Kong, Hong Kong, China
e-mail: lmlui@math.cuhk.edu.hk

K. Chen et al. (eds.), *Handbook of Mathematical Models and Algorithms in Computer Vision and Imaging*, https://doi.org/10.1007/978-3-030-98661-2_113

Abstract

Surface parameterization is of fundamental importance for many tasks in computer vision and imaging. In recent years, computational quasi-conformal geometry has become an emerging tool for the design of efficient and accurate parameterization methods for both surface meshes and point clouds. More specifically, using quasi-conformal (QC) theory, it is possible to reduce the geometric distortion and achieve conformal parameterizations for surfaces with different topology easily. It is also possible to achieve surface parameterizations that satisfy certain prescribed conditions, such as landmark constraints, with a minimal quasi-conformal distortion. In this article, we give an overview of the recent advances in surface parameterization using quasi-conformal geometry.

Keywords

Surface parameterization · Quasi-conformal geometry · Conformal map · Quasi-conformal map · Mesh · Point cloud

Introduction

Surface parameterization refers to the process of finding a one-to-one correspondence between a complicated surface and a simple parameter domain. It has widespread applications in computer graphics, vision, imaging, and also many other areas in science, engineering, and medicine, such as medical shape analysis (Zhao et al. 2019), greedy routing (Li et al. 2015), virtual broadcasting (Yueh et al. 2020), and topology optimization (Vogiatzis et al. 2018). The parameter domain depends on the topology of the given surface. For simply connected open surfaces in $\mathbb{R}^3$, common choices of the parameter domain include the unit disk, the unit square, a rectangle, or a more flexible planar domain. For multiply connected open surfaces, it is common to parameterize the surfaces onto a planar circle domain with circular holes. For genus-0 closed surfaces, it is common to use the unit sphere as the parameter domain. For other high-genus surfaces, more complicated fundamental domains are often considered. Therefore, the surface topology plays an important role in the development of surface parameterization methods. Figure 1 shows several examples of parameterization of surfaces with different topology.

Given a surface and a target parameter domain, there are numerous ways of finding a parameterization mapping from the surface onto the parameter domain. In general, it is desirable to find a low-distortion parameterization such that the geometric information of the surface is preserved as much as possible in the simple domain. However, it is well-known that isometric (distance-preserving) mappings are not possible for general surfaces. In other words, geometric distortions unavoidable exist under surface parameterization. Therefore, different distortion criteria and measures have been considered in the development of surface parameterization methods. One major class of surface parameterization methods is the conformal parameterization, which preserves angles and hence the local geometry of the

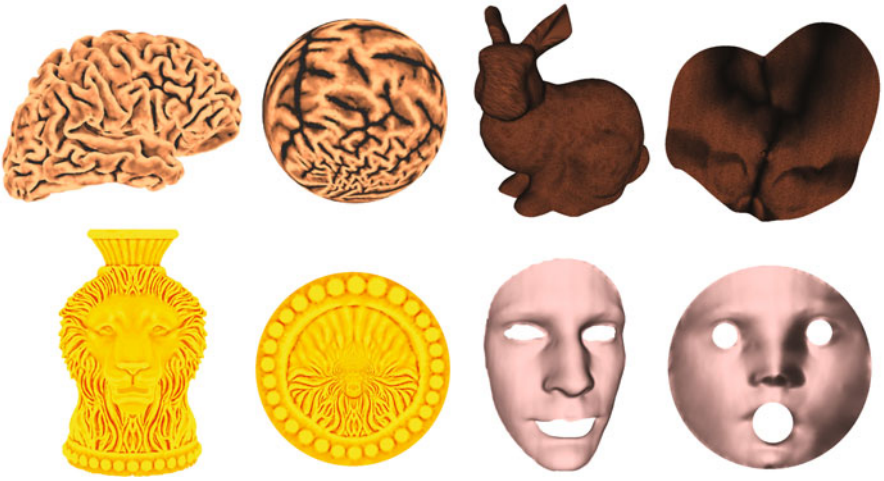

Fig. 1 Parameterization of surfaces with different topology. The top left panel shows a spherical conformal parameterization of a genus-0 closed surface. (Image adapted from Choi et al. 2015). The top right panel shows a free-boundary conformal parameterization of a simply connected open surface. (Image adapted from Choi et al. 2020a). The bottom left panel shows a disk conformal parameterization of a simply connected open surface. (Image adapted from Choi and Lui 2015). The bottom right panel shows a poly-annulus conformal parameterization of a multiply connected open surface. (Image adapted from Choi et al. 2021)

surfaces. Another major class of surface parameterization methods is the area-preserving (authalic) parameterization, which focuses on the preservation of the area elements. One may also look for parameterizations that achieve a balance between angle and area preservation or parameterizations that minimize the distortions subject to additional constraints such as prescribed landmark correspondences.

In the discrete case, surfaces are usually represented using either triangle meshes or point clouds. Each triangle mesh $\mathcal{M} = (\mathcal{V}, \mathcal{E}, \mathcal{F})$ consists of a set of vertices $\mathcal{V}$, a set of edges $\mathcal{E}$ connecting the vertices, and a set of triangular faces $\mathcal{F}$. Each point cloud $\mathcal{P}$ only consists of the vertex information but not the connectivity between the vertices. Because of the difference in the available geometric information, the developments of parameterization methods for meshes and point clouds are usually handled differently. Two examples of triangle meshes and point clouds with the parameterization results are shown in Fig. 2.

In recent years, computational quasi-conformal geometry has become a subject of great interest for the design of parameterization methods for both meshes and point clouds. Specifically, quasi-conformal theory has been utilized for reducing the conformal distortion of some prior parameterization methods to achieve conformal parameterizations. Also, for some situations where conformal parameterizations are not possible due to other prescribed constraints, quasi-conformal parameterizations with optimized conformal distortion can be obtained using computational tools based on quasi-conformal theory.

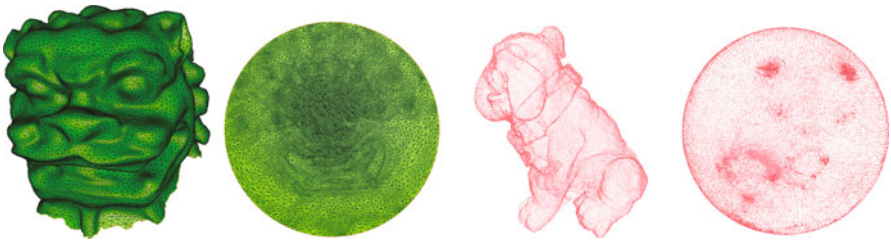

Fig. 2 Examples of mesh and point cloud parameterizations. Left: A simply connected open triangle mesh and the disk conformal parameterization. (Image adapted from Choi and Lui 2015). Right: A genus-0 point cloud and the spherical conformal parameterization. (Image adapted from Choi et al. 2016)

In this survey, we give an overview of the recent developments of surface parameterization methods using quasi-conformal geometry. Below, we first review some previous works on mesh and point cloud parameterization in section "Previous Works on Surface Parameterization". In section "Mathematical Background", we introduce the basic concepts of conformal and quasi-conformal maps. We then describe the recent advances in mesh parameterization and point cloud parameterization based on quasi-conformal geometry in sections "Mesh Parameterization Using Quasi-conformal Geometry" and "Point Cloud Parameterization Using Conformal and Quasi-conformal Geometry", respectively. In section "Applications", we review some applications of the conformal and quasi-conformal mapping methods in science, engineering, and medicine. A concluding remark is given in section "Conclusion".

Previous Works on Surface Parameterization

Mesh Parameterization

Over the past several decades, numerous mesh parameterization methods have been developed. Readers are referred to Floater and Hormann (2005), Sheffer et al. (2006), and Hormann et al. (2007) for detailed surveys on the subject. Below, we highlight some recent works on mesh parameterization.

In recent years, conformal parameterization methods have been extensively studied (see Gu and Yau 2008; Gu et al. 2020 for a comprehensive discussion). Among all conformal parameterization methods, one common approach is to make use of harmonic energy minimization (Gu et al. 2004; Lai et al. 2014). Another common approach is to utilize surface Ricci flow (Jin et al. 2008; Yang et al. 2009; Zhang et al. 2014) (see Zhang et al. 2015 for a survey). Other notable methods for computing conformal parameterizations include the slit map (Yin et al. 2008), Koebe's iteration (Zeng et al. 2009), metric scaling (Ben-Chen et al.

2008), boundary first flattening (Sawhney and Crane 2017), and conformal energy minimization (Yueh et al. 2017).

Area-preserving mesh parameterization methods have also been widely studied in recent years. Recent works include the Lie advection method (Zou et al. 2011), the optimal mass transportation (OMT) method (Zhao et al. 2013; Su et al. 2016; Nadeem et al. 2016; Pumarola et al. 2019; Giri et al. 2021; Lei and Gu 2021; Choi et al. 2022), stretch energy minimization (Yueh et al. 2019), and density-equalizing maps (Choi and Rycroft 2018; Choi et al. 2020b).

Besides, there are many other energy minimization approaches for computing mesh parameterizations in computer graphics. Typically, these approaches define some distortion measures and attempt to minimize them to produce the desired effects. Recent works include the advanced MIPS method (Fu et al. 2015), symmetric Dirichlet energy (Smith and Schaefer 2015), scalable locally injective mappings (SLIM) (Rabinovich et al. 2017), isometry-aware preconditioning (Claici et al. 2017), progressive parameterization (Liu et al. 2018), and efficient bijective parameterizations (Su et al. 2020).

Point Cloud Parameterization

With the advancement of 3D data acquisition techniques, the use of point clouds has been increasingly popular in recent decades. For this reason, there is also an increasing interest in the development of point cloud parameterization methods for the shape analysis and processing of point clouds.

In 2004, Zwicker and Gotsman proposed a spherical parameterization method for genus-0 point clouds. In 2006, Tewari et al. proposed a doubly periodic global parameterization method for genus-1 point clouds. In 2010, Zhang et al. developed an as-rigid-as-possible meshless parameterization method for point clouds with disk topology. In 2013, Meng et al. proposed a self-organizing radial basis function (RBF) neural network method for point cloud parameterization.

For the conformal parameterization of point clouds, one important component is the approximation of the Laplacian operator on point clouds. In recent years, several point cloud Laplacian approximation methods have been proposed, including the moving least squares (MLS) method (Belkin et al. 2009; Liang et al. 2012; Liang and Zhao 2013), the local mesh method (Lai et al. 2013; Choi et al. 2022), and the non-manifold Laplacian method (Sharp and Crane 2020).

Mathematical Background

In this section, we review the concepts of conformal and quasi-conformal maps. Readers are referred to Lehto (1973), Gardiner and Lakic (2000), and Ahlfors (2006) for more details.

Conformal Maps

Let $f : \mathbb{C} \to \mathbb{C}$ be a map on the complex plane $\mathbb{C}$. Write $f(z) = f(x, y) = u(x, y) + iv(x, y)$, where $z = x + iy$, i is the imaginary number with $i^2 = -1$, and u, v are real-valued functions. Suppose the derivative of f is nonzero everywhere. f is said to be *conformal* if it satisfies the Cauchy-Riemann equations:

$$\frac{\partial u}{\partial x} = \frac{\partial v}{\partial y} \quad \text{and} \quad \frac{\partial u}{\partial y} = -\frac{\partial v}{\partial x}. \tag{1}$$

If we denote the following:

$$\frac{\partial f}{\partial \overline{z}} = f_{\overline{z}} = \frac{1}{2}\left(\frac{\partial f}{\partial x} + i\frac{\partial f}{\partial y}\right) \quad \text{and} \quad \frac{\partial f}{\partial z} = f_z = \frac{1}{2}\left(\frac{\partial f}{\partial x} - i\frac{\partial f}{\partial y}\right), \tag{2}$$

then Equation (1) can be rewritten as follows:

$$\frac{\partial f}{\partial \overline{z}} = 0. \tag{3}$$

Conformal maps preserve angles and hence the local geometry. Intuitively, under a conformal map, infinitesimal circles are mapped to infinitesimal circles (see Fig. 3).

Quasi-conformal Maps

Quasi-conformal maps are a generalization of conformal maps. More specifically, an orientation-preserving homeomorphism $f : \mathbb{C} \to \mathbb{C}$ is said to be *quasi-conformal* if it satisfies the Beltrami equation:

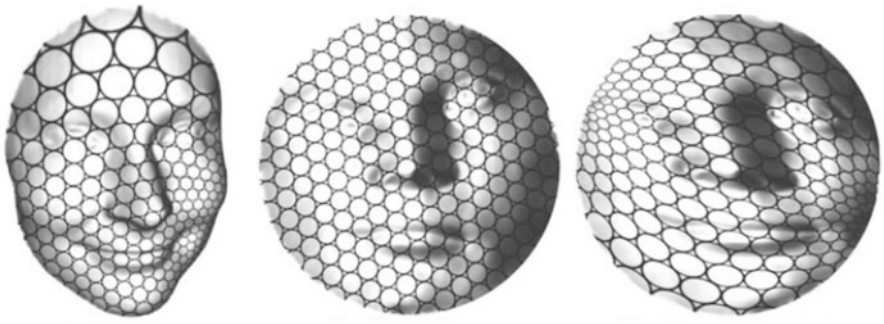

Fig. 3 An illustration of conformal and quasi-conformal maps. (Image adapted from Lui et al. 2014). Left: A surface with a circle packing texture. Middle: A conformal map of the surface onto the unit disk. Note that the small circles are mapped to small circles. Right: A quasi-conformal map of the surface onto the unit disk. Note that the small circles are mapped to small ellipses

$$\frac{\partial f}{\partial \overline{z}} = \mu_f(z)\frac{\partial f}{\partial z} \tag{4}$$

for some complex-valued function μ_f with $||\mu_f||_\infty < 1$. μ is called the *Beltrami coefficient* of the map f. Considering the first order approximation of f around a point p with respect to its local parameter, we have the following:

$$\begin{aligned} f(z) &= f(p) + f_z(p)(z-p) + f_{\overline{z}}(p)\overline{z-p} \\ &= f(p) + f_z(p)\left(z - p + \mu_f(p)\overline{z-p}\right). \end{aligned} \tag{5}$$

This gives the following:

$$\left|f(z) - f(p)\right| = \left|f_z(p)\right|\left|z - p + \mu_f(p)\overline{z-p}\right| \tag{6}$$

and hence:

$$\left|f_z(p)\right|\left(1 - \left|\mu_f(p)\right|\right)|z-p| \le |f(z) - f(p)| \le \left|f_z(p)\right|\left(1 + \left|\mu_f(p)\right|\right)|z-p|. \tag{7}$$

This shows that an infinitesimal circle is mapped to an infinitesimal ellipse with bounded eccentricity under a quasi-conformal map (see Figs. 3 and 4), where the maximal magnification factor is $\left|f_z(p)\right|\left(1 + |\mu_f(p)|\right)$, the maximal shrinkage factor is $\left|f_z(p)\right|\left(1 - \left|\mu_f(p)\right|\right)$, and the maximal dilatation of f is as follows:

$$K(f) = \frac{1 + \|\mu_f\|_\infty}{1 - \|\mu_f\|_\infty}. \tag{8}$$

Also, note that the last equality in Equation (7) holds if and only if:

$$z - p = c\mu_f(p)\overline{z-p} \tag{9}$$

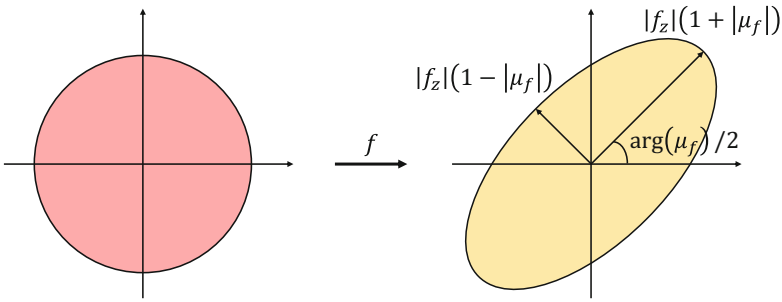

Fig. 4 An illustration of quasi-conformal maps. (Image adapted from Choi et al. 2020c)

for some $c \in \mathbb{R}$, which gives the following:

$$\arg(z-p) = \arg(\mu_f(p)) - \arg(z-p) \Leftrightarrow \arg(z-p) = \arg(\mu_f(p))/2. \tag{10}$$

This shows that the orientation change of the major axis of the ellipse is $\arg(\mu_f(p))/2$. From the above, it can be observed that the Beltrami coefficient μ encodes useful information of the quasi-conformality of the mapping f.

The bijectivity of the map f is also related to the Beltrami coefficient of it. More specifically, if $f(z) = f(x+iy) = u(x,y) + iv(x,y)$, where u, v are two real-valued functions, the Jacobian of f is given by the following:

$$\begin{aligned} J_f &= u_x v_y - u_y v_x \\ &= \frac{1}{4}\left((u_x + v_y)^2 + (u_y - v_x)^2 - (u_x - v_y)^2 - (u_y + v_x)^2\right) \\ &= \left|\frac{1}{2}(f_x - if_y)\right|^2 - \left|\frac{1}{2}(f_x + if_y)\right|^2 \\ &= |f_z|^2 - |f_{\bar{z}}|^2 \\ &= |f_z|^2 \left(1 - |\mu_f|\right)^2, \end{aligned} \tag{11}$$

which indicates that J_f is positive everywhere if $\|\mu_f\|_\infty < 1$.

The correspondence between Beltrami coefficients and quasi-conformal maps is given by the measurable Riemann mapping theorem (Gardiner and Lakic 2000):

Theorem 1 (Measurable Riemann mapping theorem). *If $\mu : \overline{\mathbb{C}} \to \overline{\mathbb{C}}$ be a Lebesgue measurable function with $\|\mu\|_\infty < 1$. There exists a quasi-conformal homeomorphism $\phi : \overline{\mathbb{C}} \to \overline{\mathbb{C}}$ in the Sobolev space $W^{1,2}(\overline{\mathbb{C}})$ satisfying the Beltrami equation (4) in the distribution sense. By fixing 0, 1, and ∞, ϕ is uniquely determined for any given μ.*

In other words, a quasi-conformal map can be uniquely determined by its associated Beltrami coefficient under suitable normalization.

Given two quasi-conformal maps $f : \Omega_1 \subset \mathbb{C} \to \Omega_2 \subset \mathbb{C}$ and $g : \Omega_2 \subset \mathbb{C} \to \Omega_3 \subset \mathbb{C}$, the Beltrami coefficient of the composition map $g \circ f$ is given by the following composition formula:

$$\mu_{g\circ f} = \frac{\mu_f + \frac{\overline{f_z}}{f_z}(\mu_g \circ f)}{1 + \frac{\overline{f_z}}{f_z}\overline{\mu_f}(\mu_g \circ f)}. \tag{12}$$

In particular, if $\mu_{f^{-1}} = \mu_g$, then:

$$\mu_f + \frac{\overline{f_z}}{f_z}(\mu_g \circ f) = \mu_f + \frac{\overline{f_z}}{f_z}(\mu_{f^{-1}} \circ f) = \mu_f + \frac{\overline{f_z}}{f_z}\left(-\frac{f_z}{\overline{f_z}}\mu_f\right) = 0, \tag{13}$$

and hence $g \circ f$ is conformal. This idea of quasi-conformal composition plays an important role in many recent parameterization methods.

To define quasi-conformal maps between two Riemann surfaces, the concept of Beltrami differential is used. More specifically, given any Riemann surface $\mathcal{S}$, a Beltrami differential $\mu(z)\frac{\overline{dz}}{dz}$ is an assignment to each chart (U_α, ϕ_α) of an L_∞ complex-valued function μ_α defined on local parameter z_α, such that:

$$\mu_\alpha \frac{\overline{dz_\alpha}}{dz_\alpha} = \mu_\beta \frac{\overline{dz_\beta}}{dz_\beta} \tag{14}$$

on the domain which is also covered by another chart (U_β, ϕ_β). Let $f : \mathcal{M} \to \mathcal{N}$ be an orientation-preserving diffeomorphism between two Riemann surfaces $\mathcal{M}, \mathcal{N}$. f is said to be quasi-conformal associated with the Beltrami differential $\mu(z)\frac{\overline{dz}}{dz}$ if for any chart (U_α, ϕ_α) on $\mathcal{M}$ and any chart (U_β, ϕ_β) on $\mathcal{N}$; the mapping $f_{\alpha\beta} := \phi_\beta \circ f \circ \phi_\alpha^{-1}$ is quasi-conformal associated with $\mu_\alpha \frac{\overline{dz_\alpha}}{dz_\alpha}$.

Linear Beltrami Solver (LBS)

As described above, there is a close relationship between Beltrami coefficients and quasi-conformal maps. It is natural to ask whether one can reconstruct a quasi-conformal map f from a given complex-valued function μ easily. To achieve this task, Lui et al. developed an efficient method called the *linear Beltrami solver* (LBS) in Lui et al. (2013). The method is outlined below.

Let $f(z) = f(x + iy) = u(x, y) + iv(x, y)$ and $\mu(z) = \rho(z) + i\tau(z)$, where u, v, ρ, τ are real-valued functions. The Beltrami equation (4) can then be rewritten as follows:

$$\mu_f = \frac{(u_x - v_y) + i(v_x + u_y)}{(u_x + v_y) + i(v_x - u_y)}. \tag{15}$$

Now, we can express v_x and v_y as linear combinations of u_x and u_y:

$$\begin{aligned} -v_y &= \alpha_1 u_x + \alpha_2 u_y; \\ v_x &= \alpha_2 u_x + \alpha_3 u_y, \end{aligned} \tag{16}$$

where:

$$\alpha_1 = \frac{(\rho - 1)^2 + \tau^2}{1 - \rho^2 - \tau^2}, \quad \alpha_2 = -\frac{2\tau}{1 - \rho^2 - \tau^2}, \quad \alpha_3 = \frac{1 + 2\rho + \rho^2 + \tau^2}{1 - \rho^2 - \tau^2}. \tag{17}$$

We can also express u_x and u_y as linear combinations of v_x and v_y similarly:

$$\begin{aligned} u_y &= \alpha_1 v_x + \alpha_2 v_y; \\ -u_x &= \alpha_2 v_x + \alpha_3 v_y. \end{aligned} \tag{18}$$

Now, since $\nabla \cdot \begin{pmatrix} -v_y \\ v_x \end{pmatrix} = 0$ and $\nabla \cdot \begin{pmatrix} u_y \\ -u_x \end{pmatrix} = 0$, we have the following:

$$\nabla \cdot \left(A \begin{pmatrix} u_x \\ u_y \end{pmatrix} \right) = 0 \text{ and } \nabla \cdot \left(A \begin{pmatrix} v_x \\ v_y \end{pmatrix} \right) = 0, \tag{19}$$

where $A = \begin{pmatrix} \alpha_1 & \alpha_2 \\ \alpha_2 & \alpha_3 \end{pmatrix}$.

In the discrete case, one can discretize the elliptic PDEs (19) as sparse positive definite linear systems. Therefore, for any given μ and some prescribed boundary conditions, one can efficiently obtain a quasi-conformal map f with the associated Beltrami coefficient being μ. See Lui et al. (2013) for more details of the computational procedure of the LBS method.

Beltrami Holomorphic Flow (BHF)

In Lui et al. (2010, 2012), Lui et al. developed another method called the *Beltrami holomorphic flow* (BHF) for reconstructing quasi-conformal maps for given Beltrami coefficients. The BHF method is based on the following theorem (Gardiner and Lakic 2000):

Theorem 2 (Beltrami holomorphic flow on $\overline{\mathbb{C}}$). *There is a 1-1 correspondence between the set of quasi-conformal maps $f : \overline{\mathbb{C}} \to \overline{\mathbb{C}}$ that fix the points $0, 1, \infty$ and the set of smooth complex-valued functions μ on $\overline{\mathbb{C}}$ with $\|\mu\|_\infty < 1$. Here, the solution f^μ to the Beltrami equation (4) depends holomorphically on μ. Let $\{\mu(t)\}$ be a family of Beltrami coefficients, where t is a real or complex parameter. Suppose $\mu(t)$ can be written in the following form:*

$$\mu(t)(z) = \mu(z) + t\nu(z) + t\epsilon(t)(z), \tag{20}$$

with μ in the unit ball of $C^\infty(\mathbb{C})$, ν, $\epsilon(t) \in L^\infty(\mathbb{C})$ such that $\|\epsilon(t)\|_\infty \to 0$ as $t \to 0$. Then, for all $w \in \mathbb{C}$, we have the following:

$$f^{\mu(t)}(w) = f^\mu(w) + tV(f^\mu, \nu)(w) + o(|t|) \tag{21}$$

locally uniformly on $\mathbb{C}$ as $t \to 0$, where:

$$V(f^{\mu}, \nu)(w) = -\frac{f^{\mu}(w)(f^{\mu}(w)-1)}{\pi} \int_{\mathbb{C}} \frac{\nu(z)(f^{\mu})_z(z))^2}{f^{\mu}(z)(f^{\mu}(z)-1)(f^{\mu}(z)-f^{\mu}(w))} dz. \tag{22}$$

In other words, given a Beltrami coefficient and the target positions of three points, one can obtain a unique quasi-conformal map. In practice, to reconstruct the quasi-conformal map, one can start with the identity map and iteratively flow the map to f^{μ} using BHF. See Lui et al. (2012) for more details of the computational procedure of the BHF method.

Teichmüller Maps

Teichmüller maps (T-maps) are a special class of quasi-conformal maps. A quasi-conformal map $f : \mathbb{C} \to \mathbb{C}$ is said to be a *Teichmüller map* if its associated Beltrami coefficient is of the following form:

$$\mu_f = k\frac{\overline{\phi}}{\phi}, \tag{23}$$

where ϕ is a complex-valued function and k is a constant with $k < 1$. In other words, the quasi-conformal distortion of a Teichmüller map is uniform over the entire domain. More generally, a quasi-conformal map $f : S_1 \to S_2$ between two Riemann surfaces is said to be a *Teichmüller map* associated with the quadratic differential $q = \varphi dz^2$ if its associated Beltrami differential is of the following form:

$$\mu_f = k\frac{\overline{\varphi}}{\varphi}, \tag{24}$$

where $\varphi : S_1 \to \mathbb{C}$ is a holomorphic function, $q \neq 0$ is a quadratic differential with $\|q\|_1 = \int_{S_1} |\varphi| < \infty$, and k is a constant with $k < 1$.

Another closely related concept is the extremal map. A quasi-conformal map $f : S_1 \to S_2$ is said to be *extremal* if for any quasi-conformal map $g : S_1 \to S_2$ isotopic to f relative to the boundary, we have the following:

$$K(f) \leq K(g). \tag{25}$$

Teichmüller maps and extremal maps are connected by the following theorem (Lui et al. 2014):

Theorem 3 (Landmark-matching Teichmüller map). *Let $g : \partial\mathbb{D} \to \partial\mathbb{D}$ be an orientation-preserving diffeomorphism of the boundary of the unit disk, with $g'(e^{i\theta}) \neq 0$ and $g''(e^{i\theta})$ is bounded for all θ. Let $\{p_j\}_{j=1}^n$ and $\{q_j\}_{j=1}^n$ be two sets of corresponding interior landmarks in $\mathbb{D}$. Then there exists a landmark-matching*

Teichmüller map $f : \mathbb{D} \to \mathbb{D}$ *that is the unique extremal extension of* g *to* $\mathbb{D}$*, i.e.,* $f|_{\partial\mathbb{D}} = g$ *and* $f(p_j) = q_j$ *for all* $j = 1, 2, \ldots, n$.

In other words, besides having uniform quasi-conformal distortion, Teichmüller maps are extremal in the sense that they minimize the maximal dilatation K.

In 2014, Lui et al. proposed a method called the *QC iteration* method for the computation of landmark-matching Teichmüller maps. The QC iteration method iteratively updates the Beltrami coefficient and reconstructs the associated quasi-conformal map using the LBS method until the resulting map becomes Teichmüller. More specifically, suppose the initial quasi-conformal map f_0 is associated with the Beltrami coefficient μ_0. The method computes the following iteratively:

$$\begin{aligned} \nu_{n+1} &:= \mathcal{A}(\mathcal{L}(\mu_n)), \\ f_{n+1} &:= \mathbf{LBS}_{\mathrm{LM}}(\nu_{n+1}), \\ \mu_{n+1} &:= \mu(f_{n+1}), \end{aligned} \tag{26}$$

until $\|\nu_{n+1} - \nu_n\|_\infty$ is less than a given stopping parameter $\epsilon > 0$. Here, $\mathcal{L}$ is the Laplacian smoothing operator, $\mathcal{A}$ is an averaging operator, $\mathbf{LBS}_{\mathrm{LM}}$ denotes the quasi-conformal map obtained by the LBS method with the prescribed landmark constraints, and $\mu(f_{n+1})$ denotes the Beltrami coefficient of f_{n+1} obtained from the Beltrami equation (4). The convergence of the QC iteration method has been proved in Lui et al. (2015).

Mesh Parameterization Using Quasi-conformal Geometry

In recent years, quasi-conformal theory has been widely used in surface mapping, registration, and visualization. For instance, Zeng et al. (2012) developed a method for computing quasi-conformal mappings between Riemann surfaces using Yamabe flow and an auxiliary metric which incorporates quasi-conformality induced from the Beltrami differential. Specifically, quasi-conformal mappings are equivalent to conformal mappings under the auxiliary metric and hence can be effectively computed. Lipman et al. (2012) computed quasi-conformal plane deformations by introducing a formula for 4-point planar warping. Weber et al. (2012) developed a method for computing piecewise linear approximations of extremal quasi-conformal maps. Lipman (2012) and Chien et al. (2016) developed methods for computing bounded distortion mappings. Wong and Zhao (2014, 2015) developed methods for computing surface mappings using discrete Beltrami flow. Zeng and Gu (2011) proposed a surface registration method using quasi-conformal curvature flow. Lui and Wen (2014) proposed a method for high-genus surface registration by computing a quasi-conformal map between the conformal embedding of the surfaces on the hyperbolic disk. Quasi-conformal theory has also been used in the development of rectilinear maps (Yang and Zeng 2020) and retinotopic maps (Tu et al. 2020; Ta

Table 1 A summary of recent mesh parameterization methods based on quasi-conformal theory

Method	Surface type	Target domain	Criterion
FLASH (Choi et al. 2015)	Topological sphere	Sphere	Conformal/ quasi-conformal
FSQC (Choi et al. 2016)	Topological sphere	Sphere	Quasi-conformal
Fast disk map (Choi and Lui 2015)	Topological disk	Disk	Conformal
Linear disk map (Choi and Lui 2018)	Topological disk	Disk	Conformal
Carotid flattening (Choi et al. 2017)	Topological disk	L-shaped	Conformal
LSQC (Qiu et al. 2019)	Topological disk	Free-boundary	Quasi-conformal
PGCP (Choi et al. 2020a)	Simply connected	Free/disk/sphere	Conformal
ACM/PACM (Choi et al. 2021)	Multiply connected	Circle domain	Conformal
QCMC (Ho and Lui 2016)	Multiply connected	Circle domain	Quasi-conformal
BHF (Ng et al. 2014)	Multiply connected	Circle domain	Teichmüller

et al. 2021). In this section, we review the latest mesh parameterization methods developed based on quasi-conformal geometry.

By the uniformization theorem, every simply connected Riemann surface is conformally equivalent to either the unit disk, the complex plane, or the Riemann sphere. Also, every multiply connected open surface is conformally equivalent to a circle domain with circular holes. Therefore, as mentioned earlier in section "Introduction", various methods have been proposed for parameterizing surface meshes with different topology onto different parameter domains. Table 1 summarizes the recent mesh parameterization methods based on quasi-conformal theory. Below, we first introduce the parameterization methods for genus-0 closed triangle meshes and then discuss the methods for simply connected and multiply connected open triangle meshes.

Genus-0 Closed Triangle Meshes

Conformal Parameterization

In 2015, Choi et al. proposed a fast algorithm for the spherical conformal parameterization of genus-0 closed triangle meshes (see Fig. 5). More specifically, given a genus-0 closed triangle mesh $\mathcal{M}$, the algorithm first follows the idea in Haker et al. (2000) and punctures one triangle $T = [v_i, v_j, v_k]$ from $\mathcal{M}$. The punctured surface $\mathcal{M} \setminus T$ is then a simply connected open surface and hence can be mapped onto the plane by solving the Laplace equation:

$$\Delta g = 0, \tag{27}$$

where $g : \mathcal{M} \setminus T \to \mathbb{C}$ flattens the punctured mesh onto a planar triangular domain with the three mapped boundary vertices $g(v_i)$, $g(v_j)$, and $g(v_k)$ forming a

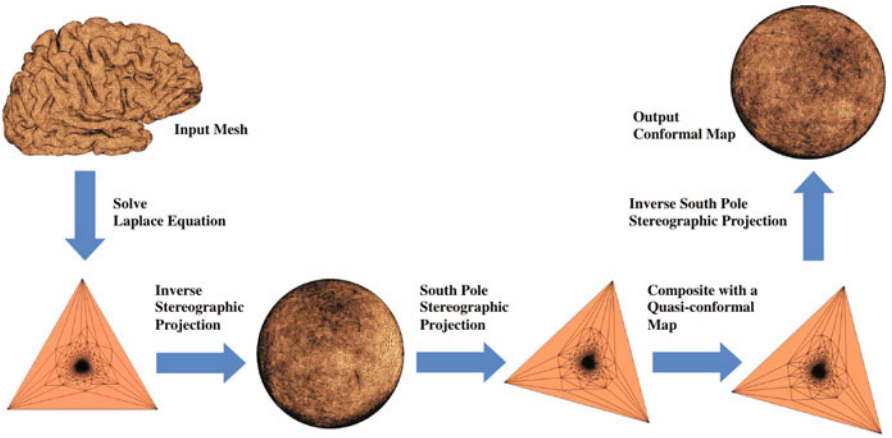

Fig. 5 An illustration of the fast spherical conformal parameterization method. (Image adapted from Choi et al. 2015)

boundary triangle with the same angle structure as T. One can then map the planar triangular domain onto the unit sphere using the inverse stereographic projection $\varphi_N^{-1} : \overline{\mathbb{C}} \to \mathbb{S}^2$, where the stereographic projection $\varphi_N : \mathbb{S}^2 \to \overline{\mathbb{C}}$ is given by the following:

$$\varphi_N(X, Y, Z) = \frac{X}{1-Z} + i\frac{Y}{1-Z} \tag{28}$$

and the inverse stereographic projection $\varphi_N^{-1} : \overline{\mathbb{C}} \to \mathbb{S}^2$ is given by the following:

$$\varphi_N^{-1}(z) = \left(\frac{2\mathrm{Re}(z)}{1+|z|^2}, \frac{2\mathrm{Im}(z)}{1+|z|^2}, \frac{1-|z|^2}{1+|z|^2} \right). \tag{29}$$

The composition map $\varphi_N^{-1} \circ g$ is then a parameterization mapping from $\mathcal{M}$ onto the unit sphere $\mathbb{S}^2$. However, the conformal distortion near the punctured triangle T, which corresponds to the north pole region of the unit sphere, is severe in the discrete case. To correct the conformal distortion there, the algorithm in Choi et al. (2015) maps the sphere to the extended complex plane using the south pole stereographic projection $\varphi_S : \mathbb{S}^2 \to \overline{\mathbb{C}}$ with the following:

$$\varphi_S(X, Y, Z) = \frac{X}{1+Z} + i\frac{Y}{1+Z}, \tag{30}$$

such that the south pole region of the unit sphere is mapped to the outermost part of the planar domain and the north pole region of the unit sphere is mapped to the innermost part of the planar domain. The algorithm then computes a quasi-conformal map $h : \mathbb{C} \to \mathbb{C}$ with the Beltrami coefficient $\mu_h = \mu_{(\varphi_S \circ \varphi_N^{-1} \circ g)^{-1}}$ and

with the outermost part of the domain fixed using the LBS method (Lam and Lui 2014). The composition map $h \circ \varphi_S \circ \varphi_N^{-1} \circ g$ is then conformal by the composition formula in Equation (12). Finally, the map $\varphi_S^{-1} \circ h \circ \varphi_S \circ \varphi_N^{-1} \circ g$ gives a conformal parameterization of $\mathcal{M}$ onto the unit sphere. Moreover, the use of the Beltrami coefficients also helps ensure that the mapping is bijective (see Fig. 6).

Another spherical conformal parameterization method that utilizes quasi-conformal theory is the parallelizable global conformal parameterization (PGCP) method (Choi et al. 2020a) (see Fig. 7 for an example). The PGCP method achieves the conformal parameterization using a divide-and-conquer manner by considering

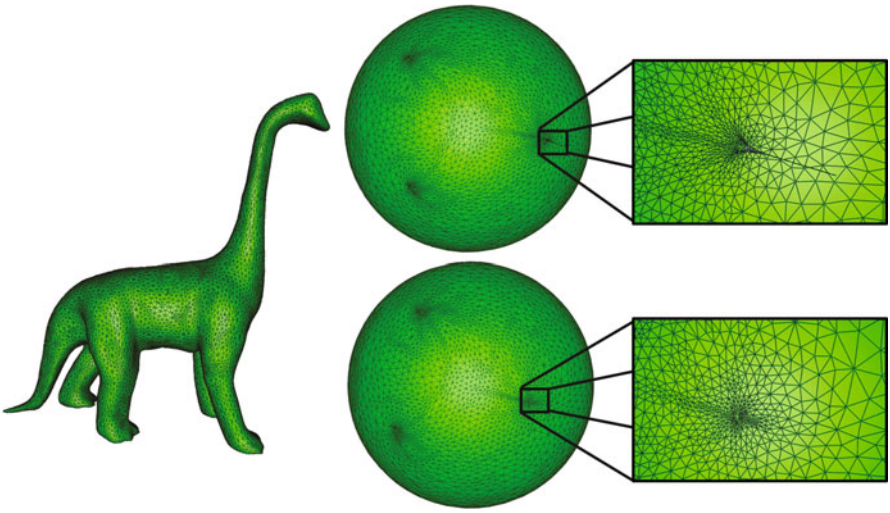

Fig. 6 The spherical conformal parameterization method in Choi et al. (2015) is capable of mapping a complicated dinosaur mesh (left) onto the unit sphere bijectively (bottom right), while the traditional method (Gu et al. 2004) (top right) produces overlaps. (Image adapted from Choi 2016)

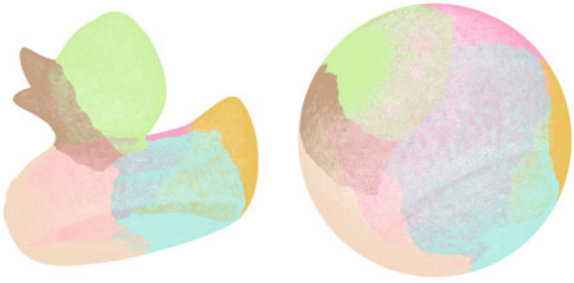

Fig. 7 The spherical conformal parameterization of a genus-0 duck surface mesh obtained using the parallelizable global conformal parameterization (PGCP) method. (Image adapted from Choi et al. 2020a). The colors indicate the correspondence between the subdomains in the original mesh and in the parameterization result

a partition of the input triangle mesh into several submeshes. Because of the use of mesh partition, the PGCP method is capable of handling not only genus-0 closed surfaces but also simply connected open surfaces. The method will be explained in detail later in section "Simply Connected Open Triangle Meshes".

Quasi-conformal Parameterization

In 2015, Choi et al. developed the fast landmark-aligned spherical harmonic parameterization (FLASH) method for genus-0 closed triangle meshes (see Fig. 8 for an illustration). More specifically, given two genus-0 closed triangle meshes $\mathcal{S}_1$ and $\mathcal{S}_2$ with two sets of corresponding landmarks $\{p_j\}_{j=1}^n$ and $\{q_j\}_{j=1}^n$ on $\mathcal{S}_1$ and $\mathcal{S}_2$, respectively, denote the spherical conformal parameterization of $\mathcal{S}_2$ obtained by the abovementioned method in Choi et al. (2015) by $\phi_2 : \mathcal{S}_2 \to \mathbb{S}^2$. The FLASH method aims to find a spherical parameterization $f : \mathcal{S}_1 \to \mathbb{S}^2$ such that $f(p_j)$ matches $\phi_2(q_j)$ as accurately as possible for all $j = 1, 2, \ldots, n$, and the conformal distortion of f is also as small as possible. To achieve this, the method first computes the spherical conformal parameterization $\phi_1 : \mathcal{S}_1 \to \mathbb{S}^2$. It then solves for a quasi-conformal map $\psi : \mathbb{S}^2 \to \mathbb{S}^2$ that minimizes the following combined energy:

$$E_{\text{combined}}(\psi) = \int |\nabla \psi|^2 + \lambda \sum_{j=1}^{n} |\psi(\phi_1(p_j)) - \phi_2(q_j)|^2, \tag{31}$$

where $\lambda \geq 0$ is a weighting factor for balancing the conformality and the landmark mismatch. In particular, a large λ yields a quasi-conformal map with a smaller landmark mismatch but a larger conformal distortion, while a small λ yields a smaller conformal distortion but the landmark mismatch will be larger. ϕ can be obtained by solving the following equation:

$$\Delta \psi + \lambda \delta_E(\psi - \phi_2(q_j)) = 0, \tag{32}$$

where $\delta_E(w)$ is the smooth approximation of the characteristic function:

$$\chi_E(w) = \begin{cases} 1 & \text{if } w = \phi_2(q_j) \text{ for some } j, \\ 0 & \text{otherwise.} \end{cases} \tag{33}$$

The desired landmark-aligned spherical parameterization is then given by $f = \psi \circ \phi_1$. The bijectivity of the parameterization can be further enforced by modifying the norm of the Beltrami coefficient and reconstructing the associated quasi-conformal map iteratively. Figure 9 shows for some examples of landmark-aligned spherical parameterization obtained using the FLASH method.

In 2016, Choi et al. developed the fast spherical quasi-conformal parameterization (FSQC) method for the computation of spherical parameterization of genus-0

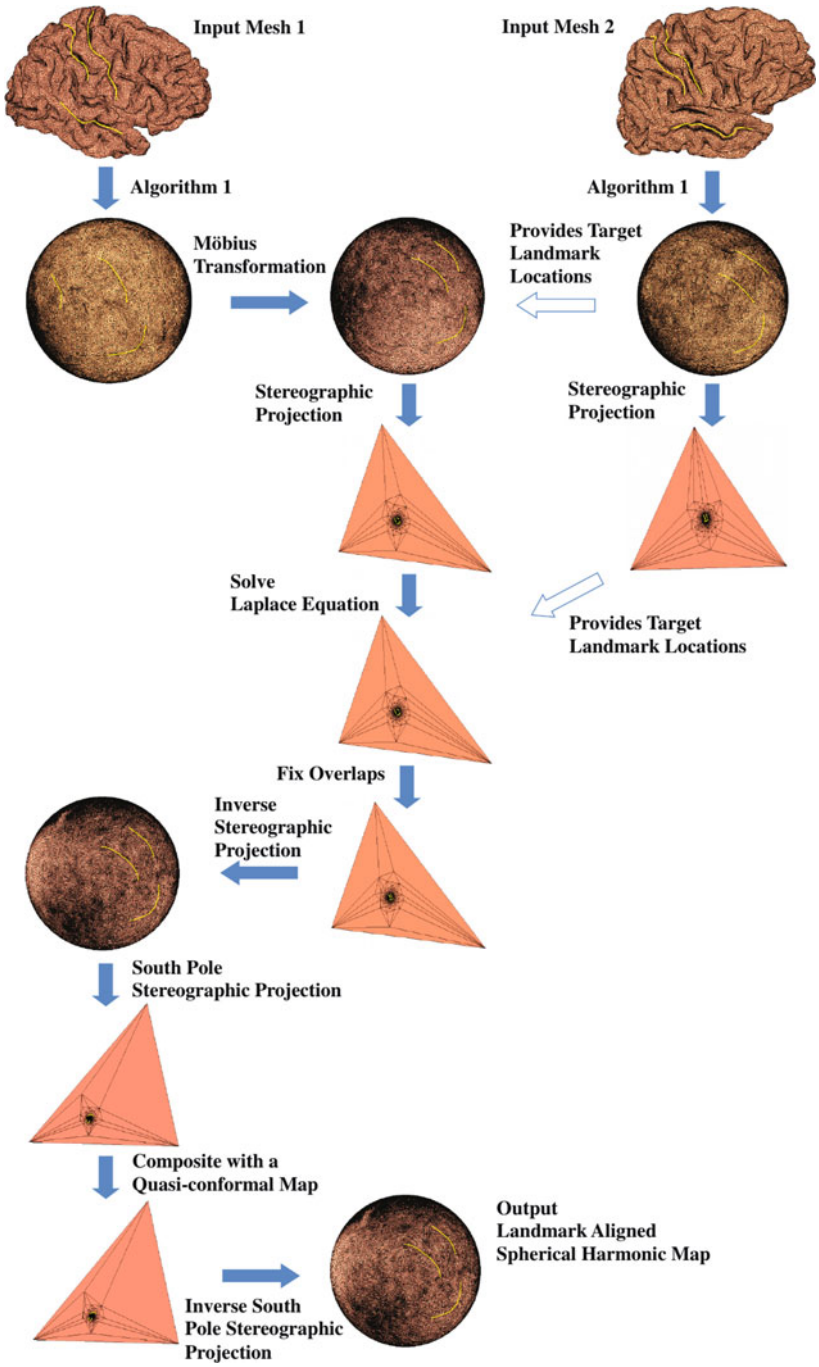

Fig. 8 An illustration of the fast landmark-aligned spherical harmonic parameterization (FLASH) method. (Image adapted from Choi et al. 2015)

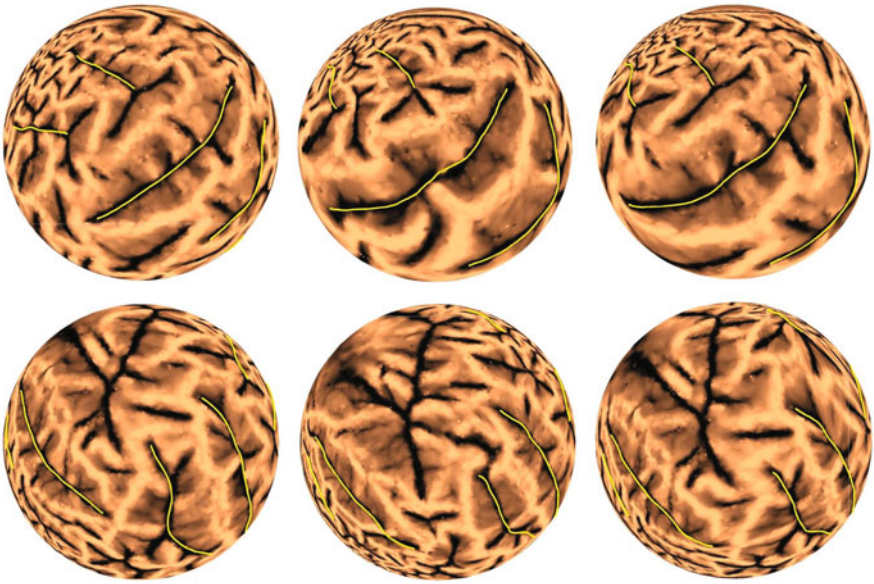

Fig. 9 Two examples of the landmark-constrained spherical quasi-conformal parameterization obtained using the FLASH method. (Image adapted from Choi et al. 2015). Each row shows an example. Left column: The spherical conformal parameterization of the source mesh. Middle column: The spherical conformal parameterization of the target mesh. Right column: The landmark-constrained quasi-conformal parameterization

closed triangle meshes with a prescribed quasi-conformal dilatation. Specifically, given any genus-0 closed triangle mesh $\mathcal{M} = (\mathcal{V}, \mathcal{E}, \mathcal{F})$ and a user-defined quasi-conformal dilatation $K : \mathcal{F} \to \mathbb{R}$ defined on every triangular face of the mesh, the method starts by computing the spherical conformal parameterization of $\mathcal{M}$ using the method in Choi et al. (2015). Next, it searches for a triangle T on the spherical parameterization such that both T and its neighboring faces are the most regular and then performs a stereographic projection with respect to T to map the sphere onto the plane. Then, to achieve the prescribed dilatation K, the method constructs a Beltrami coefficient μ with the following:

$$\mu(T) = \frac{K(T) - 1}{K(T) + 1} \tag{34}$$

for every triangle T. By applying the LBS method (Lui et al. 2013) to reconstruct a quasi-conformal map on the plane associated with the Beltrami coefficient μ followed by the inverse stereographic projection, the desired spherical quasi-conformal parameterization is obtained. Figure 10 shows an example of spherical quasi-conformal parameterization obtained by the FSQC method.

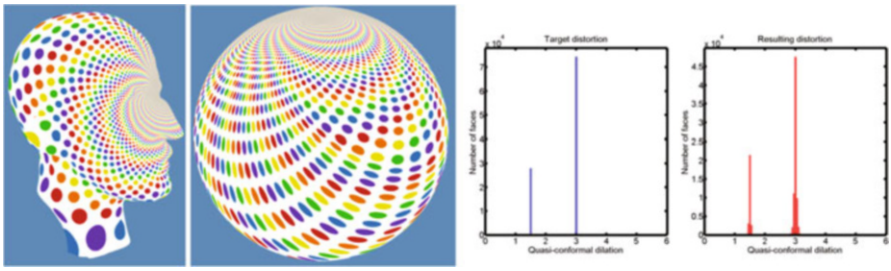

Fig. 10 An example of the fast spherical quasi-conformal parameterization (FSQC) method for genus-0 closed triangle meshes. (Image adapted from Choi et al. 2016). Left: The input genus-0 closed surface with a circle packing texture and the spherical quasi-conformal parameterization obtained by FSQC. Right: The prescribed quasi-conformal dilatation and the final dilatation of the resulting parameterization. Note that the circles on the input surface are mapped to two classes of ellipses with different eccentricity as shown in the parameterization result, which correspond to $K = 1.5$ and $K = 3$ in the target dilatation histogram, respectively

Simply Connected Open Triangle Meshes

Conformal Parameterization

In 2015, Choi and Lui proposed a fast disk conformal parameterization method for simply connected open triangle meshes (see Fig. 11). The method involves two major steps, namely, the "north pole" step and the "south pole" step. Analogous to the spherical conformal parameterization method in Choi et al. (2015), the method handles the conformal distortion at different parts of the parameter domain separately. More specifically, after getting an initial disk harmonic map by solving the Laplace equation:

$$\Delta f = 0 \tag{35}$$

subject to a circular boundary constraint, the method considers the following "north pole" step. It first maps the unit disk to the upper half plane using the Cayley transform:

$$W(z) = i\frac{1+z}{1-z}, \tag{36}$$

and composes the map with another quasi-conformal map to reduce the conformal distortion using the idea of quasi-conformal composition in Equation (12) with the boundary triangle fixed. Then, it maps the upper half plane back to the unit disk using the inverse Cayley transform:

$$W^{-1}(z) = \frac{z-i}{z+i}. \tag{37}$$

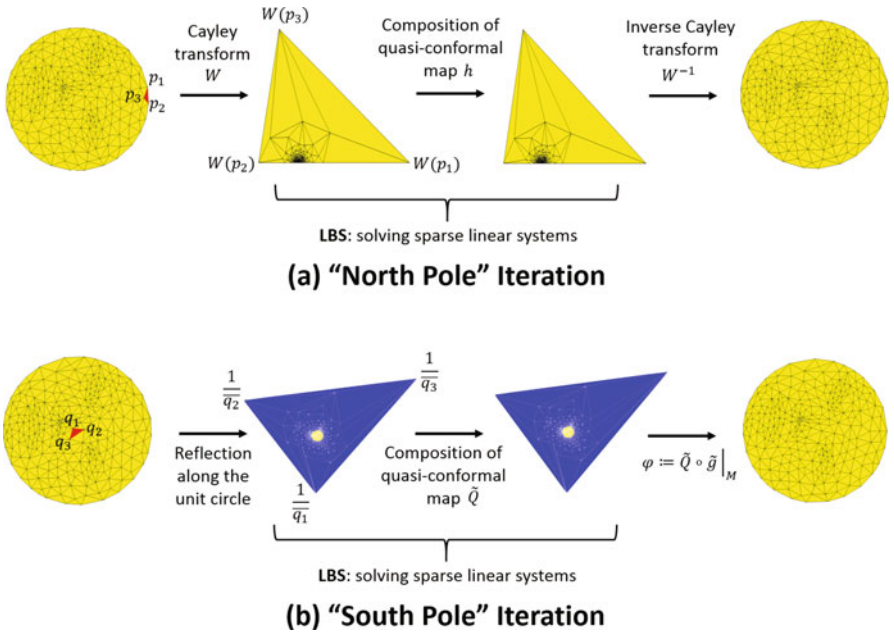

Fig. 11 An illustration of the fast disk conformal parameterization method for simply connected open triangle meshes. (Image adapted from Choi and Lui 2015). (**a**) "North pole" iteration. (**b**) "South pole" iteration

The above step helps reduce the conformal distortion at the innermost region of the disk, while the distortion at the region around $z = 1$ may still be large. Therefore, in the subsequent "south pole" step, the method uses a reflection mapping $z \mapsto \frac{1}{\bar{z}}$ to reflect the disk along the unit circle, so that the outermost region of the new shape corresponds to the innermost region of the disk, which is with low conformal distortion due to the previous "north pole" step. One can then fix the outermost region and apply the idea of quasi-conformal composition again to compute a quasi-conformal map so that the conformal distortion at the region around $z = 1$ is reduced. By repeating the above procedure, one can eventually obtain a disk conformal parameterization.

In 2018, Choi and Lui proposed a linear formulation for disk conformal parameterization of simply connected open triangle meshes. The idea is to use a technique called *double covering* to turn any given simply connected open triangle mesh into a genus-0 mesh and then apply the fast spherical conformal parameterization method in Choi et al. (2015). More specifically, given a simply connected open triangle mesh $\mathcal{M} = (\mathcal{V}, \mathcal{E}, \mathcal{F})$, the method constructs a new mesh $\mathcal{M}'$ by duplicating $\mathcal{M}$ and reversing the orientation of every triangle in it. In other words, for each triangle $[v_i, v_j, v_k]$ in $\mathcal{M}$, the corresponding triangle in $\mathcal{M}$ is given by $[v_i', v_k', v_j']$, where v_i', v_j', v_k' are copies of the vertices v_i, v_j, v_k. One can then glue $\mathcal{M}$ and $\mathcal{M}'$

along their boundaries $\partial\mathcal{M}$ and $\partial\mathcal{M}'$ by identifying all the corresponding boundary vertices. The glued surface (denoted by $\tilde{\mathcal{M}}$) is then a genus-0 closed triangle mesh. Hence, one can apply the fast spherical conformal parameterization method in Choi et al. (2015) for parameterizing $\tilde{\mathcal{M}}$. By extracting the part corresponding to $\mathcal{M}$ in the spherical parameterization and applying the stereographic projection in Equation (28), we obtain a conformal parameterization of $\mathcal{M}$ onto a planar domain. As the planar domain may not be perfectly circular, the method further enforces the circularity of the boundary using a projection:

$$v \mapsto \frac{v}{|v|} \tag{38}$$

for all boundary vertices. Finally, to correct the conformal distortion caused by the projection, the method composes the parameterization map with another quasi-conformal map based on the composition formula in Equation (12), thereby yielding a disk conformal parameterization (see Fig. 12 for an example).

Note that the abovementioned methods compute the conformal parameterization of the input mesh globally. In case the density of the input mesh is very high or the mesh geometry is complicated, the computation of the global parameterization may be expensive and challenging. To resolve this issue, Choi et al. (2020a) proposed the parallelizable global conformal parameterization (PGCP) method (Choi et al. 2020a) (see Fig. 13 for an illustration). Specifically, the PGCP method considers partitioning the input mesh into different subdomains. For each subdomain, the discrete natural conformal parameterization (DNCP) method in Desbrun et al. (2002) is used for finding an initial free-boundary conformal flattening map. As the local parameterizations of different subdomains may not be consistent along their boundaries, the PGCP method looks for a series of conformal maps to deform

Fig. 12 The disk conformal parameterization of a simply connected open surface obtained using the linear disk map method. (Image adapted from Choi and Lui 2018)

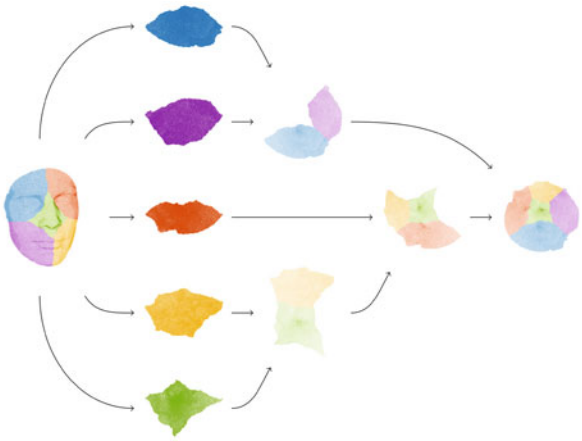

Fig. 13 An illustration of the parallelizable global conformal parameterization (PGCP) method. (Image adapted from Choi et al. 2020a)

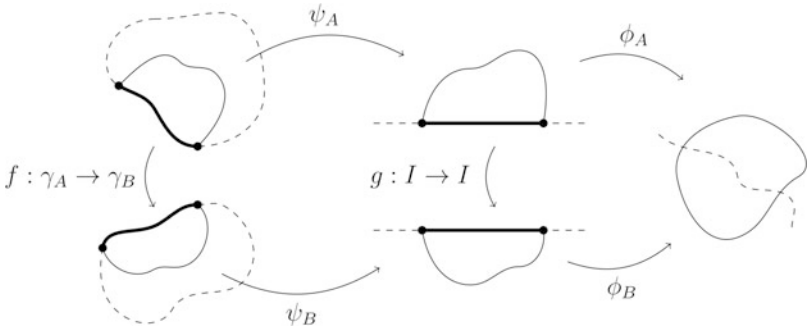

Fig. 14 An illustration of the partial welding procedure. (Image adapted from Choi et al. 2020a)

the boundaries to enforce the consistency between them. This is achieved using a variant of conformal welding called *partial welding*.

More specifically, given a diffeomorphism f from a closed curve (e.g., the unit circle) to itself, conformal welding aims to find two Jordan domains $D, \Omega \subset \overline{\mathbb{C}}$ and two conformal maps $\phi : D \to \Omega$ and $\phi^* : D^* \to \Omega^*$, where D^* and Ω^* are the exterior of D and Ω, respectively, such that $\phi = \phi^* \circ f$ on the closed curve. In other words, the two surfaces are stitched together seamlessly. By the sewing theorem (Lehto 1973), if f is a quasisymmetric function from the real axis to itself, then the upper and lower half-planes can be mapped conformally onto disjoint Jordan domains D, Ω by two maps ϕ, ϕ^*, with $\phi(x) = \phi^*(f(x))$ for all $x \in \mathbb{R}$. Partial welding is a variant of conformal welding in the sense that it does not assume the full correspondence between two boundary curves but only the correspondence between a portion of the two curves. As illustrated in Fig. 14, to enforce the consistency between two arcs of the boundaries of two Jordan regions A and B on the complex plane, one can apply a series of analytic functions to map A to the upper half plane and B to the lower half plane such that the two corresponding arcs are mapped to the same interval I on the real axis. Then, one can

find a conformal map that matches the corresponding points on the two arcs, thereby enforcing the consistency between them. After transforming all the boundaries of the flattened subdomains using this idea of partial welding, one can solve the Laplace equation subject to the welded boundary constraints for each subdomain. The final result is then a global free-boundary conformal parameterization of the input mesh. It is noteworthy that both the initial and final parameterizations of the subdomains are independent of those of the other subdomains, and hence one can exploit parallelization in the computational procedure. Some additional steps can be further incorporated for producing disk conformal parameterizations. It is also possible to further reduce the area distortion of the conformal parameterizations by finding an optimal Möbius transformation.

For some applications, it is more desirable to compute conformal parameterizations of the given surfaces onto a standardized planar domain different from a disk or a rectangle. For instance, 3D carotid artery surfaces are usually visualized with the aid of a nonconvex L-shaped parameter domain. In 2017, Choi et al. developed a conformal parameterization method for flattening carotid artery surface meshes. The method starts by computing an arclength scaling map onto a nonconvex L-shaped planar domain for the initialization. Next, it computes the Beltrami coefficient of the inverse of the arclength scaling map and then constructs a quasi-conformal map from the L-shaped domain onto itself with the same Beltrami coefficient using the LBS method (Lui et al. 2013), thereby yielding a conformal flattening map by the composition formula in Equation (12). However, since the L-shaped domain is nonconvex, the overall mapping is not guaranteed to be bijective especially near the nonconvex corner of the domain. To enforce the bijectivity, the method considers smoothing and chopping the Beltrami coefficient iteratively. More specifically, the smoothing step is done by solving the following energy minimization problem:

$$\tilde{\mu} = \text{argmin}_{\mu} \int (|\nabla \mu|^2 + |\mu - \nu| + |\mu|^2), \tag{39}$$

where ν is the current Beltrami coefficient and $\tilde{\mu}$ is the smoothed Beltrami coefficient. The chopping step is done by changing the norm of the Beltrami coefficient from $|\tilde{\mu}|$ to $\min\{|\tilde{\mu}|, 1 - \epsilon\}$ where ϵ is a small positive number. One can then reconstruct a quasi-conformal map from $\tilde{\mu}$ using the LBS method (Lui et al. 2013) and repeat the above steps until the resulting map becomes bijective. Figure 15 shows an example of the conformal parameterization of a carotid artery surface obtained by Choi et al. (2017), from which it can be observed that the parameterization facilitates the visualization of the vessel-wall-plus-plaque thickness (VWT) measurement for the carotid model.

Quasi-conformal Parameterization

The LBS method (Lui et al. 2013) and the BHF method (Lui et al. 2012) can be naturally applied for computing quasi-conformal parameterizations of any given simply connected open triangle mesh. Specifically, after parameterizing the given mesh onto a planar domain using the abovementioned conformal parameterization methods, one can compute a quasi-conformal map with a prescribed Beltrami

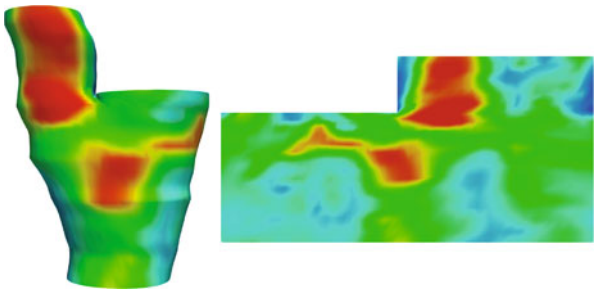

Fig. 15 The conformal parameterization of a carotid artery surface onto a standardized L-shaped planar domain. (Image adapted from Choi et al. 2017). Here, the color represents the vessel-wall-plus-plaque thickness (VWT) measurement for the carotid model

coefficient subject to some boundary constraints using either LBS or BHF. Similarly, the QC iteration method (Lui et al. 2014) can be used for computing landmark-matching Teichmüller parameterization of simply connected open triangle meshes. It is noteworthy that these approaches can only produce fixed-boundary quasi-conformal parameterizations.

More recently, Qiu et al. (2019) proposed a method for computing free-boundary quasi-conformal parameterization of simply connected open triangle meshes. Let $f(z) = f(x+iy) = u(x,y) + iv(x,y)$ and $\mu = \rho + i\tau$. The least squares quasi-conformal energy is defined as follows:

$$E_{\text{LSQC}}(u, v; \mu) = \frac{1}{2}\int_{\Omega} \|P\nabla u + JP\nabla v\|^2 dx\,dy, \tag{40}$$

where:

$$P = \frac{1}{\sqrt{1-|\mu|^2}}\begin{pmatrix} 1-\rho & -\tau \\ -\tau & 1+\rho \end{pmatrix} \tag{41}$$

and:

$$J = \begin{pmatrix} 0 & -1 \\ 1 & 0 \end{pmatrix}. \tag{42}$$

It has been shown in Qiu et al. (2019) that:

$$\begin{aligned} E_{\text{LSQC}}(u, v; \mu) = {} & \frac{1}{2}\int_{\Omega} \|A^{1/2}u\|^2 dx\,dy + \frac{1}{2}\int_{\Omega} \|A^{1/2}v\|^2 dx\,dy \\ & - \int_{\Omega} (u_y v_x - u_x v_y) dx\,dy, \end{aligned} \tag{43}$$

where:

$$A = \begin{pmatrix} \frac{(\rho-1)^2+\tau^2}{1-\rho^2-\tau^2} & -\frac{2\tau}{1-\rho^2-\tau^2} \\ -\frac{2\tau}{1-\rho^2-\tau^2} & \frac{1+2\rho+\rho^2+\tau^2}{1-\rho^2-\tau^2}. \end{pmatrix} \tag{44}$$

Based on this observation, the computation of a free-boundary quasi-conformal parameterization can be done in a similar manner as in the least squares conformal mapping method (Lévy et al. 2002; Desbrun et al. 2002).

Multiply Connected Open Triangle Meshes

Conformal Parameterization

In Choi et al. (2021), Choi developed a method for the annulus conformal parameterization of multiply connected open triangle meshes with one hole and a method for the poly-annulus conformal parameterization of multiply connected open triangle meshes with $k > 1$ holes.

An illustration of the annulus conformal map (ACM) method is shown in Fig. 16. Given any multiply connected open triangle mesh, the ACM method starts by finding a path from a vertex at the inner boundary to a vertex at the outer boundary and slicing the mesh along the path. As the sliced mesh is simply connected, one can map it onto a rectangle using the rectangular conformal parameterization method in Meng et al. (2016) with a periodic boundary constraint at the top and bottom boundaries (the method will be explained in detail later in section "Point Cloud Parameterization Using Conformal and Quasi-conformal Geometry"). Now, denote the rectangular domain as $[0, L] \times [0, 1]$. One can apply the following exponential map η to map the rectangular domain to an annulus with inner radius $e^{-2\pi L}$ and outer radius 1:

$$\eta(z) = e^{2\pi(z-L)}. \tag{45}$$

Because of the periodic boundary constraint in the computation of the rectangular parameterization, the top and bottom boundaries of the rectangular domain will be

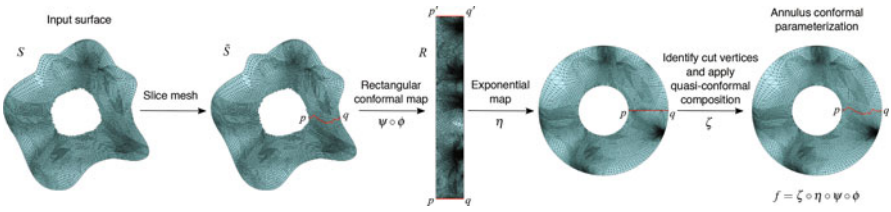

Fig. 16 An illustration of the annulus conformal map (ACM) method. (Image adapted from Choi et al. 2021)

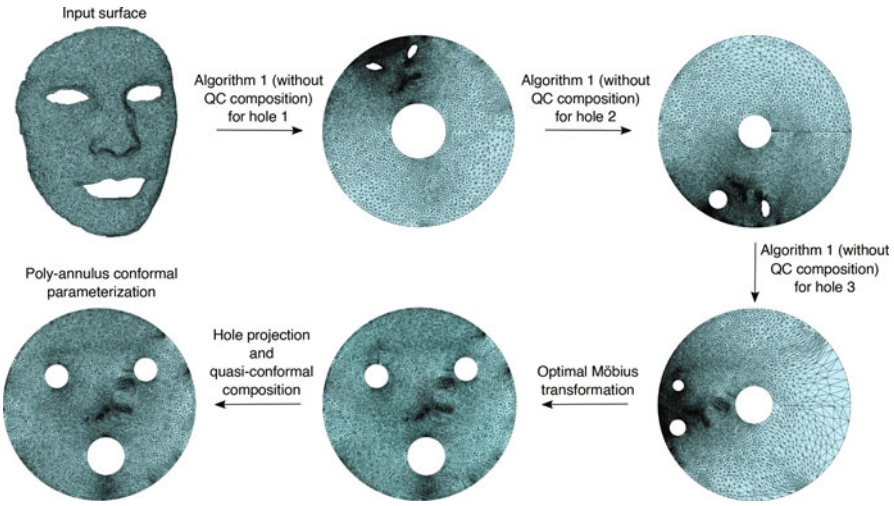

Fig. 17 An illustration of the poly-annulus conformal map (PACM) method. (Image adapted from Choi et al. 2021)

mapped to consistent positions in the annulus. Therefore, it is possible to identify the cut vertices to obtain a parameterization with annulus topology. Finally, one can apply the idea of quasi-conformal composition in Equation (12) to further reduce the conformal distortion of the parameterization caused by the cut and obtain the final annulus conformal parameterization.

Given any multiply connected open triangle mesh with $k > 1$ holes, the poly-annulus conformal map (PACM) method can be used for computing a conformal parameterization of it onto a circle domain with k circular holes (see Fig. 17 for an illustration). The PACM method starts by filling all but one holes of the input mesh and computing an initial parameterization onto an annulus, thereby making the unfilled hole circular. It then removes all filled regions and repeats the above procedure with another hole chosen to be unfilled. Under the series of annulus parameterizations, all holes eventually become highly circular in the parameter domain. Finally, the method performs a projection to further enforce the circularity of all holes and then applies the quasi-conformal composition as in Equation (12) to produce a poly-annulus conformal parameterization.

Quasi-conformal Parameterization

Given any multiply connected open surface and any target Beltrami coefficient, it is natural to ask whether one can compute a quasi-conformal parameterization of the surface onto a canonical circle domain with the Beltrami coefficient of the resulting mapping matching the input Beltrami coefficient. One major challenge in this problem is that the radii and centers of the inner circles on the circle domain

depend on the input multiply connected surface and hence cannot be set arbitrarily. As the LBS method (Lui et al. 2013) and the BHF method (Lui et al. 2012) require fixed (Dirichlet) boundary conditions, they cannot be used for computing the quasi-conformal parameterization with the desired Beltrami coefficient directly. To solve this problem, Ho and Lui (2016) proposed a variational approach called QCMC for computing the quasi-conformal parameterization of multiply connected open surfaces. More specifically, given any multiply connected open triangle mesh $\mathcal{M}$ with $\partial M = \gamma_0 - \gamma_1 - \gamma_2 - \cdots - \gamma_k$, i.e., γ_0 is the outer boundary and $\gamma_1, \ldots, \gamma_k$ are the inner boundaries, and any Beltrami coefficient μ, the QCMC method treats the radii $\mathbf{r}$ and centers $\mathbf{c}$ of the inner circles on the circle domain as variables and minimizes the following energy to solve for an optimal quasi-conformal map f:

$$E(f, \mathbf{r}, \mathbf{c}) = \int_{\mathcal{M}} \left| f_{\bar{z}} - \mu f_z \right|^2, \tag{46}$$

subject to the constraints $f(\gamma_0) = \partial\mathbb{D}$, $f(\gamma_i) = \partial\mathcal{B}_{r_i}(c_i)$ for $i = 1, \ldots, k$ and $\|\mu(f)\|_\infty = \|f_{\bar{z}}/f_z\|_\infty < 1$. Here, $\mathcal{B}_{r_i}(c_i)$ denotes the circle centered at a point $c_i \in \mathbb{Z}$ with radius $r_i > 0$. In other words, the QCMC method simultaneously searches for the optimal conformal module $(\mathbf{r}, \mathbf{c})$ for the boundary constraints and the optimal quasi-conformal map f that satisfies the boundary constraints and is associated with the prescribed Beltrami coefficient. Figure 18 shows an example of the quasi-conformal parameterization obtained by the QCMC method.

It is also possible to compute the Teichmüller parameterizations of multiply connected open triangle meshes. In 2014, Ng et al. developed a method for computing the extremal Teichmüller map between two multiply connected domains. The method iteratively updates the Beltrami coefficient of the mapping using BHF until the norm of the Beltrami coefficient becomes uniform (see Fig. 19 for an example). By combining the conformal parameterization methods for multiply connected open surfaces and the proposed extremal Teichmüller mapping method, the Teichmüller parameterization of any multiply connected open triangle mesh can be obtained.

Point Cloud Parameterization Using Conformal and Quasi-conformal Geometry

In recent years, several methods have been proposed for computing the conformal and quasi-conformal parameterization of point clouds. Many of these methods are motivated by prior mesh parameterization approaches, with some key modifications and extensions for handling point clouds. Table 2 gives an overview of the recent works. Below, we introduce the works for the parameterization of genus-0 point clouds and then the works for point clouds with disk topology.

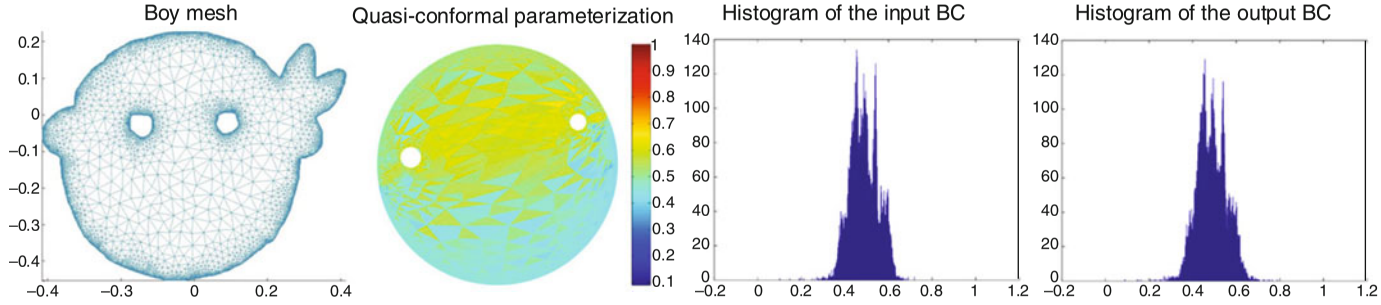

Fig. 18 An example of the QCMC method for the quasi-conformal parameterization of multiply connected open surfaces. (Image adapted from Ho and Lui 2016). Left: The input multiply connected open triangle mesh and the output quasi-conformal parameterization color-coded by the norm of the Beltrami coefficient of the output map. Right: The histograms of the norm of the prescribed Beltrami coefficient and that of the output map

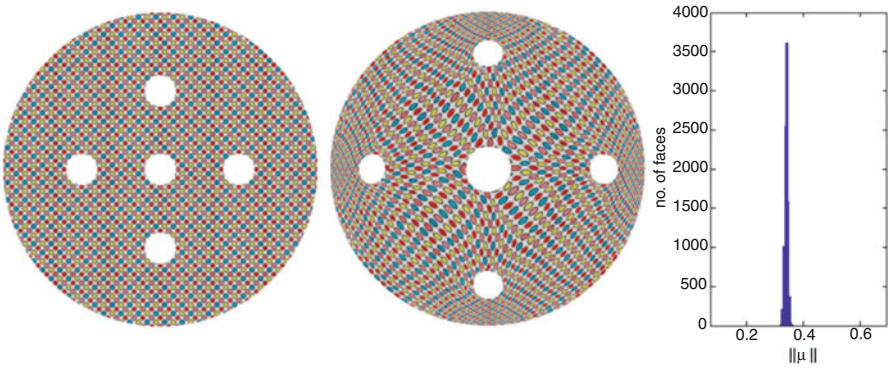

Fig. 19 An example of the extremal Teichmüller map between two multiply connected domains. (Image adapted from Ng et al. 2014). Left: A multiply connected domain with a circle packing texture. Middle: The extremal Teichmüller map onto another multiply connected domain. Note that the small circles are mapped to small ellipses with uniform eccentricity. Right: The histogram of the norm of the Beltrami coefficient of the resulting map

Table 2 A summary of recent conformal and quasi-conformal parameterization methods for point clouds

Method	Surface type	Target domain	Criterion
Spherical map (Choi et al. 2016)	Topological sphere	Sphere	Conformal
TEMPO (Meng et al. 2016)	Topological disk	Rectangle	Conformal/Teichmüller
PCQC (Meng and Lui 2018)	Topological disk	Rectangle	Quasi-conformal
Free-boundary map (Choi et al. 2022)	Topological disk	Free-boundary	Conformal

Genus-0 Point Clouds

For the parameterization of genus-0 point clouds, Choi *et al.* developed a spherical conformal parameterization method in Choi et al. (2016). Analogous to the spherical conformal mapping algorithm for triangle meshes in Choi et al. (2015), the point cloud spherical conformal parameterization method considers a "north pole" step and a "south pole" step. More specifically, the method starts by approximating the Laplacian operator on point clouds using the moving least squares (MLS) method with a Gaussian-type weight function. Using the point cloud Laplacian, one can compute a harmonic flattening map of a genus-0 point cloud and then map it to the sphere using the inverse stereographic projection in Equation (29). This forms the "north pole" step in the proposed method (Choi et al. 2016). As for the "south pole" step, instead of solving for a quasi-conformal map as described in Choi et al. (2015), here the method applies the south pole stereographic projection in Equation (30) and then solves another Laplace equation followed by the inverse south pole

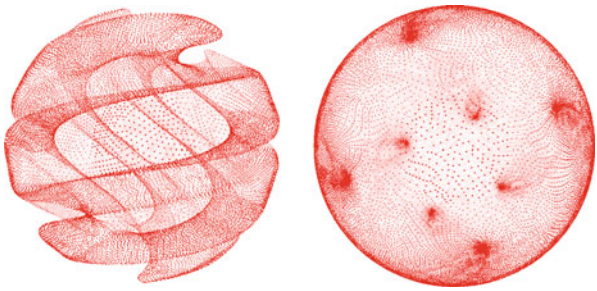

Fig. 20 Spherical conformal parameterization of genus-0 point clouds. (Image adapted from Choi et al. 2016)

stereographic projection. It was shown in Choi et al. (2016) that by performing the "north pole" step and the "south pole" step iteratively, one can eventually obtain a spherical conformal parameterization of the point cloud. In other words, using the north-south reiteration scheme, one can achieve conformality without computing quasi-conformal maps as in the abovementioned mesh parameterization methods. Figure 20 shows an example of the spherical conformal parameterization obtained by Choi et al. (2016). More recently, a variation of the method has been proposed in Jarvis et al. (2021) for the spherical parameterization of sparse genus-0 point clouds.

Point Clouds with Disk Topology

In 2016, Meng et al. proposed a framework called TEMPO for computing Teichmüller extremal mappings of point clouds with disk topology. In particular, they developed methods for computing the rectangular conformal parameterizations and landmark-matching Teichmüller parameterizations of disk-type point clouds (see Fig. 21 for an illustration).

For the rectangular conformal parameterization, the method starts by computing a harmonic map $\phi_0 : \mathcal{P} \to \mathbb{D}$ of the input disk-type point cloud $\mathcal{P}$ onto the unit disk by solving the Laplace equation:

$$\Delta \phi_0 = 0 \tag{47}$$

subject to a circular boundary constraint. It then computes a map $\phi_1 : \mathbb{D} \to [0,1]^2$ from the unit disk to the unit square by solving the generalized Laplace equation (19). Now, let $\phi_1(x,y) = u(x,y) + iv(x,y)$. To achieve conformality, the method considers rescaling the height of the square by a factor h such that the Beltrami coefficient of the map $\phi_2(x,y) = u(x,y) + ihv(x,y)$ is the same as $\mu(\phi_0^{-1})$. The optimal h is obtained by solving the following minimization problem:

$$h = \operatorname{argmin} \int_{\mathbb{D}} |\mu(\phi_2) - \mu(\phi_0^{-1})|^2. \tag{48}$$

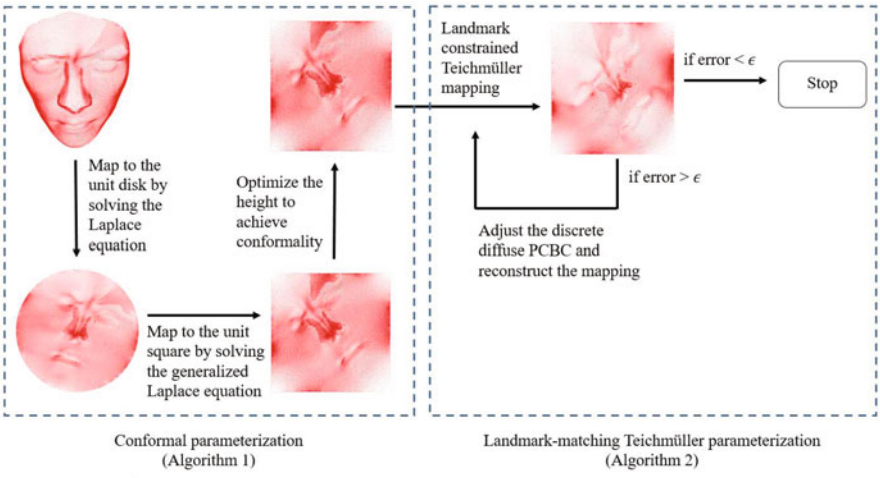

Fig. 21 The computation of rectangular conformal parameterization and landmark-matching Teichmüller parameterizations of point clouds with disk topology. (Image adapted from Meng et al. 2016)

By the composition formula (12), the composition map $\phi_2 \circ \phi_0$ with the optimal h gives a rectangular conformal parameterization of the input point cloud. After getting the rectangular conformal parameterization, the landmark-matching Teichmüller parameterization can be obtained by extending the QC iteration method (Lui et al. 2014) for point clouds. Using the TEMPO framework, it is possible to compute landmark-matching registrations of point cloud surfaces. Figure 22 shows an example of registering two facial point clouds with prescribed landmark constraints.

One important component in the above framework is the approximation of the Beltrami coefficient μ on point clouds. In 2018, Meng and Lui presented a rigorous treatment of the approximation of quasi-conformal maps and the relevant concepts on point clouds. In particular, they proposed a geometric quantity called the *point cloud Beltrami coefficient* (PCBC) and proved that it can effectively capture the local geometric distortion of a point cloud mapping. Using the PCBC, they developed the point cloud quasi-conformal (PCQC) parameterization method for the parameterization of point clouds with any prescribed PCBC (see Fig. 23 for an example).

More recently, Liu et al. developed a free-boundary conformal parameterization method for disk-type point clouds (Choi et al. 2022) by extending the mesh-based DNCP algorithm in Desbrun et al. (2002). The method approximates the Laplacian operator on disk-type point clouds using a modified local mesh method with some special treatments at the point cloud boundary. More specifically, let $\mathcal{P}$ be the given point cloud with n vertices. For each vertex v_i, the method considers its k-nearest neighbors and computes the local Delaunay triangulation to obtain a one-ring neighborhood R_i. The angles in R_i are then used for constructing an $n \times n$ matrix $L_{k,i}^{pc}$:

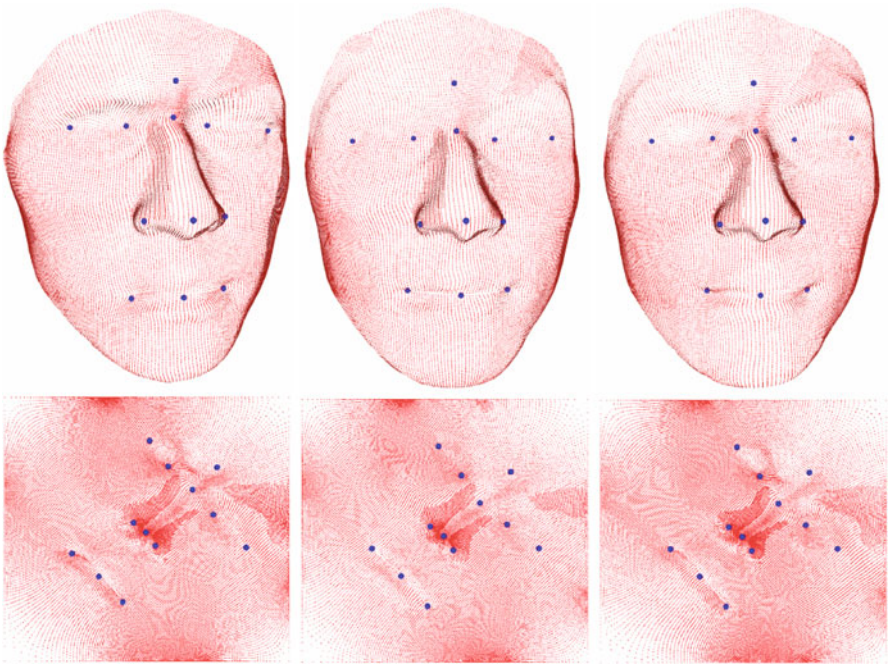

Fig. 22 An illustration of the TEMPO framework. (Image adapted from Meng et al. 2016). Left column: The source human facial point cloud and the rectangular conformal parameterization. Middle column: The target human facial point cloud and the rectangular conformal parameterization. Right column: The registration result and the corresponding landmark-matching Teichmüller mapping of the rectangular domain

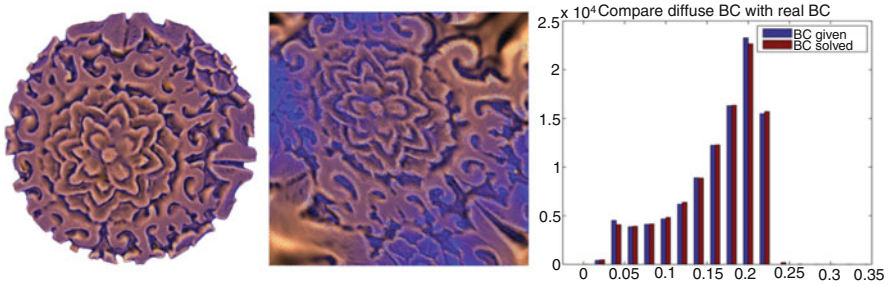

Fig. 23 An example of the point cloud quasi-conformal (PCQC) parameterization. (Image adapted from Meng and Lui 2018). Left: The input point cloud and its underlying surface. Middle column: The PCQC parameterization with the prescribed PCBC. Right: The histogram of the norm of the PCBC of parameterization result and that of the actual PCBC prescribed

$$\begin{cases} L_{k,i}^{pc}(i,j) = L_{k,i}^{pc}(j,i) = -\dfrac{1}{2}(\cot\alpha_{ij} + \cot\beta_{ij}) \quad \text{if } v_j \in R_i, \\ L_{k,i}^{pc}(i,i) = \dfrac{1}{2} \displaystyle\sum_{j:v_j \in R_i} (\cot\alpha_{ij} + \cot\beta_{ij}), \end{cases} \tag{49}$$

where α_{ij} and β_{ij} are the angles opposite to the edge $[v_i, v_j]$ in the local triangulation, and all other entries of $L_{k,i}^{pc}$ are set to be 0. Noticing that the above approximation may be inaccurate at the boundary vertices in case the point cloud boundary shape is nonconvex, the method further checks if every boundary angle θ in the local triangulation for boundary vertices satisfies the angle criterion $c_1 < \theta < c_2$, where (c_1, c_2) is a prescribed angle range. It then removes all triangles that violate this angle criterion and obtains the matrices $L_{k,i}^{pc}$ for the boundary vertices. The Laplacian operator L_k^{pc} for the entire point cloud can then be approximated by $L_k^{pc} = \frac{1}{3}\sum_{i=1}^{n} L_{k,i}^{pc}$. Finally, the point cloud parameterization $f = (f_x, f_y)$ can be obtained by solving the following linear system:

$$\left(\begin{pmatrix} L_k^{pc} & 0 \\ 0 & L_k^{pc} \end{pmatrix} - \begin{pmatrix} 0 & M_1 \\ M_2 & 0 \end{pmatrix} \right) \begin{pmatrix} f_x \\ f_y \end{pmatrix} = 0, \tag{50}$$

where $M_1(i,j) = M_2(j,i) = \frac{1}{2}$ and $M_1(j,i) = M_2(i,j) = -\frac{1}{2}$ if v_i, v_j are adjacent boundary points with positive orientation and 0 otherwise. As for the boundary conditions, the farthest two points in $\mathcal{P}$ are mapped to $(0,0)$ and $(1,0)$ following the original DNCP formulation (Desbrun et al. 2002). Moreover, it has been shown in Choi et al. (2022) that the partial welding method for triangle meshes in Choi et al. (2020a) can be extended for point cloud parameterization (see Fig. 24). More specifically, the proposed point cloud parameterization method partitions the point cloud into several subdomains and flattens the boundary of each of them onto the plane. It then applies the partial welding method to enforce the consistency of the boundaries. Finally, the interior part of each subdomain can be mapped onto the plane by solving the Laplace equation with the welded boundary constraints.

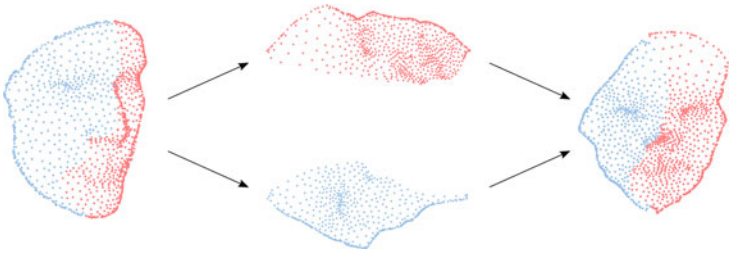

Fig. 24 An illustration of the free-boundary conformal parameterization method for disk-type point clouds via partial welding. (Image adapted from Choi et al. 2022)

Applications

The surface mapping and parameterization methods developed based on quasi-conformal geometry have been found useful in many practical applications in recent years.

For instance, the mapping methods have been applied to biological and medical shape analysis. In Zeng et al. (2010) and Zeng and Yang (2014), Zeng et al. applied quasi-conformal mappings for supine and prone colon registration. In 2015, Wen et al. used landmark-matching quasi-conformal mappings for analyzing vestibular systems. In 2015, Lam et al. used Teichmüller mappings for skull registration. In 2015, Choi et al. used the FLASH method for registering brain cortical surfaces (see Fig. 25). In Chan et al. (2016, 2020), Chan et al. utilized conformal and quasi-conformal mappings for the shape analysis of hippocampal surfaces. The spherical

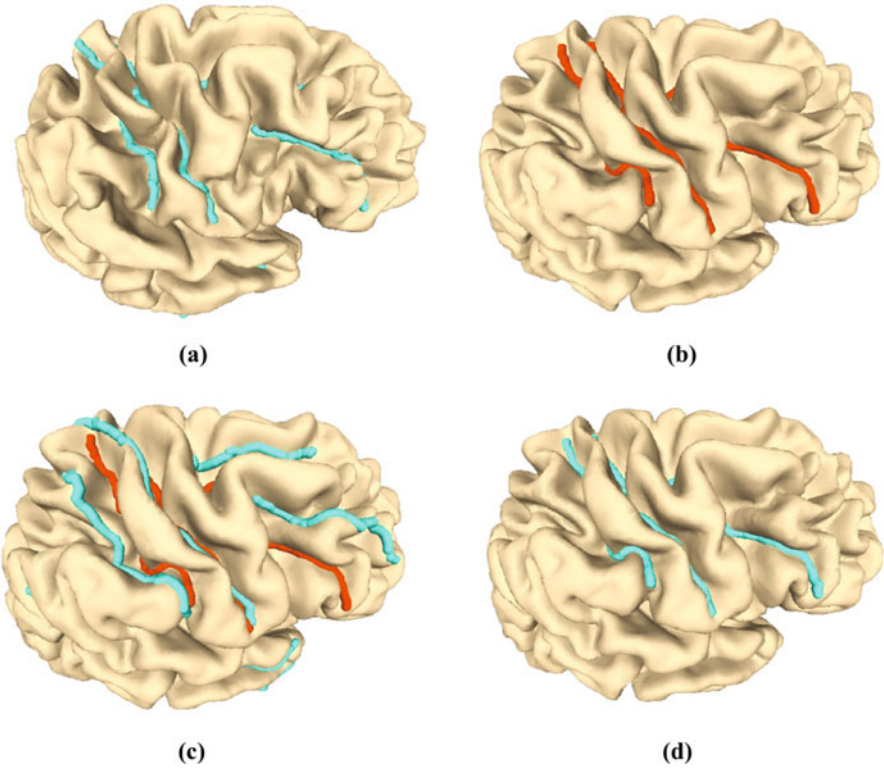

Fig. 25 Registering brain cortical surfaces using the FLASH method. (Image adapted from Choi et al. 2015). (**a**) The source brain with sulcal landmarks. (**b**) The target brain with sulcal landmarks. (**c**) The registration obtained using conformal parameterization without landmark constraints. (**d**) The registration obtained using landmark-constrained optimized conformal parameterization. It can be observed that the landmark-constrained parameterization gives a more accurate registration result

conformal parameterization method developed in Choi et al. (2015) has been applied to optical mapping for cardiac electrophysiology (Christoph et al. 2017) and cardiac radiofrequency catheter ablation (Zhou et al. 2016). In 2018, Choi and Mahadevan utilized Teichmüller mappings for insect wing morphometry (see Fig. 26). In Choi et al. (2020c,d), Choi et al. utilized conformal parameterizations and Teichmüller mappings for analyzing human and other mammalian tooth shape (see Fig. 27).

The mapping methods have also been applied to different engineering problems. For instance, the spherical conformal parameterization method in Choi et al. (2015) has been applied to collaborative robotics (Popov and Klimchik 2019). The disk conformal parameterization method in Choi and Lui (2015) has been applied to

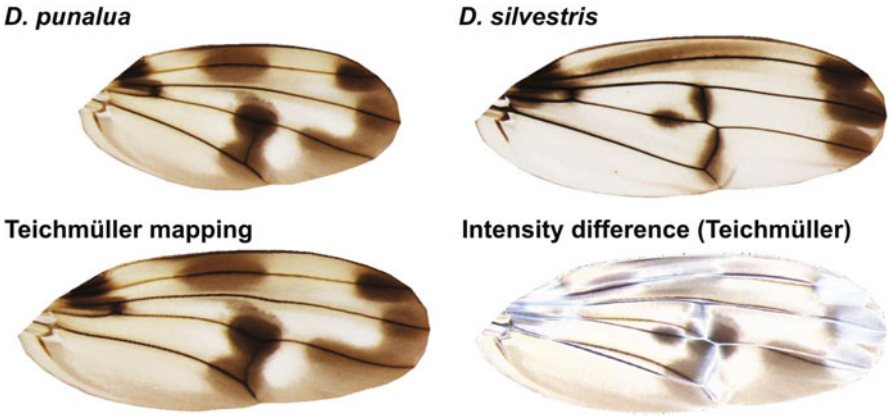

Fig. 26 Insect wing morphometry using landmark-matching Teichmüller mappings. (Image adapted from Choi and Mahadevan 2018). To quantify the difference between two different Drosophila wing shapes (top row), one can compute a landmark-matching Teichmüller mapping (bottom left) from the first wing to the second wing that matches the prominent structural features of the two wings such as the intersections of the veins. It is then possible to compare the Teichmüller mapping result and the second wing by considering their intensity difference

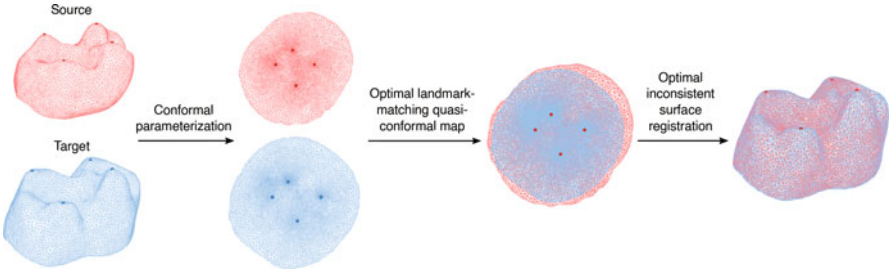

Fig. 27 Mammalian tooth morphometry using quasi-conformal mappings. (Image adapted from Choi et al. 2020c). Given two tooth surfaces, the method first computes a free-boundary conformal parameterization of each surface. It then finds an optimal landmark-matching quasi-conformal map on the plane, which finally gives an optimal inconsistent surface registration

structural optimization (Kussmaul et al. 2019) and robot navigation (Notomista and Saveriano 2021). The rectangular parameterization method in Meng et al. (2016) has been applied to T-spline surface reconstruction (Wang 2021) and nanotechnology (Guralnik 2021). In 2017, Choi et al. developed a method for subdivision connectivity surface remeshing via Teichmüller mappings. In 2018, Yung et al. developed an efficient image registration method using coarse triangulations and landmark-matching quasi-conformal mappings. In (2019, 2021), Choi et al. utilized conformal and quasi-conformal mapping methods (Meng et al. 2016; Choi and Lui 2018) in developing constrained optimization frameworks for kirigami metamaterial design. In 2021, Shaqfa et al. extended the disk conformal parameterization method (Choi and Lui 2015) for spherical cap parameterization and utilized it for analyzing stone microstructures. Recently, Jarvis et al. (2021) developed a method for reconstructing 3D asteroid and comet shapes from sparse feature point sets via spherical parameterizations based on the method in Choi et al. (2016).

Conclusion

With the theoretical guarantee and computational efficiency of quasi-conformal maps, many conformal and quasi-conformal parameterization methods have been developed for triangle meshes and point clouds. The methods have been successfully applied to various science and engineering problems.

More recently, there is an increasing interest in volumetric mapping methods for the deformations of 3D solid shapes (Lee et al. 2016; Yueh et al. 2019; Choi and Rycroft 2021; Zhang et al. 2022). Therefore, a natural future research direction is the development of higher-dimensional parameterization methods using higher-dimensional quasi-conformal theory.

Acknowledgments This work was supported in part by the National Science Foundation under Grant No. DMS-2002103 (to Gary P. T. Choi) and HKRGC GRF under project ID 2130549 (to Lok Ming Lui).

References

Ahlfors, L.V.: Lectures on Quasiconformal Mappings, vol. 38. American Mathematical Society, Providence (2006)

Belkin, M., Sun, J., Wang, Y.: Constructing Laplace operator from point clouds in $\mathbb{R}^d$. In: Proceedings of the Twentieth Annual ACM-SIAM Symposium on Discrete Algorithms, pp. 1031–1040 (2009)

Ben-Chen, M., Gotsman, C., Bunin, G.: Conformal flattening by curvature prescription and metric scaling. Comput. Graph. Forum **27**(2), 449–458 (2008)

Chan, H.L., Li, H., Lui, L.M.: Quasi-conformal statistical shape analysis of hippocampal surfaces for Alzheimer's disease analysis. Neurocomputing **175**, 177–187 (2016)

Chan, H.L., Yam, T.C., Lui, L.M.: Automatic characteristic-calibrated registration (ACC-REG): hippocampal surface registration using eigen-graphs. Pattern Recogn. **103**, 107142 (2020)

Chien, E., Levi, Z., Weber, O.: Bounded distortion parametrization in the space of metrics. ACM Trans. Graph. **35**(6), 1–16 (2016)
Choi, P.T.: Surface conformal/quasi-conformal parameterization with applications. In: CUHK Electronic Theses and Dissertations Collection, The Chinese University of Hong Kong (2016)
Choi, P.T., Lui, L.M.: Fast disk conformal parameterization of simply-connected open surfaces. J. Sci. Comput. **65**(3), 1065–1090 (2015)
Choi, G.P.-T., Lui, L.M.: A linear formulation for disk conformal parameterization of simply-connected open surfaces. Adv. Comput. Math. **44**(1), 87–114 (2018)
Choi, G.P.T., Mahadevan, L.: Planar morphometrics using Teichmüller maps. Proc. R. Soc. A **474**(2217), 20170905 (2018)
Choi, G.P.T., Rycroft, C.H.: Density-equalizing maps for simply connected open surfaces. SIAM J. Imaging Sci. **11**(2), 1134–1178 (2018)
Choi, G.P.T., Rycroft, C.H.: Volumetric density-equalizing reference map with applications. J. Sci. Comput. **86**(3), 41 (2021)
Choi, P.T., Lam, K.C., Lui, L.M.: FLASH: fast landmark aligned spherical harmonic parameterization for genus-0 closed brain surfaces. SIAM J. Imaging Sci. **8**(1), 67–94 (2015)
Choi, G.P.-T., Ho, K.T., Lui, L.M.: Spherical conformal parameterization of genus-0 point clouds for meshing. SIAM J. Imaging Sci. **9**(4), 1582–1618 (2016)
Choi, G.P.-T., Man, M.H.-Y., Lui, L.M.: Fast spherical quasiconformal parameterization of genus-0 closed surfaces with application to adaptive remeshing. Geom. Imaging Comput. **3**(1–2), 1–29 (2016)
Choi, G.P.T., Chen, Y., Lui, L.M., Chiu, B.: Conformal mapping of carotid vessel wall and plaque thickness measured from 3D ultrasound images. Med. Biol. Eng. Comput. **55**(12), 2183–2195 (2017)
Choi, C.P., Gu, X., Lui, L.M.: Subdivision connectivity remeshing via Teichmüller extremal map. Inverse Probl. Imaging **11**(5), 825–855 (2017)
Choi, G.P.T., Dudte, L.H., Mahadevan, L.: Programming shape using kirigami tessellations. Nat. Mater. **18**(9), 999–1004 (2019)
Choi, G.P.T., Leung-Liu, Y., Gu, X., Lui, L.M.: Parallelizable global conformal parameterization of simply-connected surfaces via partial welding. SIAM J. Imaging Sci. **13**(3), 1049–1083 (2020a)
Choi, G.P.T., Chiu, B., Rycroft, C.H.: Area-preserving mapping of 3D carotid ultrasound images using density-equalizing reference map. IEEE Trans. Biomed. Eng. **67**(9), 1507–1517 (2020b)
Choi, G.P.T., Qiu, D., Lui, L.M.: Shape analysis via inconsistent surface registration. Proc. R. Soc. A **476**(2242), 20200147 (2020c)
Choi, G.P.T., Chan, H.L., Yong, R., Ranjitkar, S., Brook, A., Townsend, G., Chen, K., Lui, L.M.: Tooth morphometry using quasi-conformal theory. Pattern Recogn. **99**, 107064 (2020d)
Choi, G.P.T.: Efficient conformal parameterization of multiply-connected surfaces using quasi-conformal theory. J. Sci. Comput. **87**(3), 70 (2021)
Choi, G.P.T., Giri, A., Kumar, L.: Adaptive area-preserving parameterization of open and closed anatomical surfaces. Comput. Biol. Med., **148**, 105715 (2022)
Choi, G.P.T., Dudte, L.H., Mahadevan, L.: Compact reconfigurable kirigami. Phys. Rev. Res. **3**(4), 043030 (2021)
Choi, G.P.T., Liu, Y., Lui, L.M.: Free-boundary conformal parameterization of point clouds. J. Sci. Comput. **90**(1), 14 (2022)
Christoph, J., Schröder-Schetelig, J., Luther, S.: Electromechanical optical mapping. Prog. Biophys. Mol. Biol. **130**, 150–169 (2017)
Claici, S., Bessmeltsev, M., Schaefer, S., Solomon, J.: Isometry-aware preconditioning for mesh parameterization. Comput. Graph. Forum **36**(5), 37–47 (2017)
Desbrun, M., Meyer, M., Alliez, P.: Intrinsic parameterizations of surface meshes. Comput. Graph. Forum **21**(3), 209–218 (2002)
Floater, M.S., Hormann, K.: Surface parameterization: a tutorial and survey. In: Advances in Multiresolution for Geometric Modelling, pp. 157–186. Springer, Berlin/New York (2005)
Fu, X.-M., Liu, Y., Guo, B.: Computing locally injective mappings by advanced MIPS. ACM Trans. Graph. **34**(4), 1–12 (2015)

Gardiner, F.P., Lakic, N.: Quasiconformal Teichmüller Theory, vol. 76. American Mathematical Society, Providence (2000)
Giri, A., Choi, G.P.T., Kumar, L.: Open and closed anatomical surface description via hemispherical area-preserving map. Sig. Process. **180**, 107867 (2021)
Gu, X.D., Yau, S.-T.: Computational Conformal Geometry, vol. 1. International Press, Somerville (2008)
Gu, X., Wang, Y., Chan, T.F., Thompson, P.M., Yau, S.-T.: Genus zero surface conformal mapping and its application to brain surface mapping. IEEE Trans. Med. Imaging **23**(8), 949–958 (2004)
Gu, X., Luo, F., Yau, S.T.: Computational conformal geometry behind modern technologies. Not. Am. Math. Soc. **67**(10), 1509–1525 (2020)
Guralnik, B., Hansen, O., Henrichsen, H.H., Caridad, J.M., Wei, W., Hansen, M.F., Nielsen, P.F., Petersen, D.H.: Effective electrical resistivity in a square array of oriented square inclusions. Nanotechnology **32**(18), 185706 (2021)
Haker, S., Angenent, S., Tannenbaum, A., Kikinis, R., Sapiro, G., Halle, M.: Conformal surface parameterization for texture mapping. IEEE Trans. Vis. Comput. Graph. **6**(2), 181–189 (2000)
Ho, K.T., Lui, L.M.: QCMC: quasi-conformal parameterizations for multiply-connected domains. Adv. Comput. Math. **42**(2), 279–312 (2016)
Hormann, K., Lévy, B., Sheffer, A.: Mesh parameterization: theory and practice. In: ACM SIGGRAPH 2007 Courses (2007)
Jarvis, B., Choi, G.P.T., Hockman, B., Morrell, B., Bandopadhyay, S., Lubey, D., Villa, J., Bhaskaran, S., Bayard, D., Nesnas, I.A.: 3D shape reconstruction of small bodies from sparse features. IEEE Robot. Autom. Lett. **6**(4), 7089–7096 (2021)
Jin, M., Kim, J., Luo, F., Gu, X.: Discrete surface Ricci flow. IEEE Trans. Vis. Comput. Graph. **14**(5), 1030–1043 (2008)
Wang, J., Leach, R., Chen, R., Xu, J., Jiang, X.J.: Distortion-free intelligent sampling of sparse surfaces via locally refined T-spline metamodelling. Int. J. Precis. Eng. Manuf. – Green Technol. **8**(5), 1471–1486 (2021)
Kussmaul, R., Jónasson, J.G., Zogg, M., Ermanni, P.: A novel computational framework for structural optimization with patched laminates. Struct. Multidiscipl. Optim. **60**(5), 2073–2091 (2019)
Lai, R., Liang, J., Zhao, H.-K.: A local mesh method for solving PDEs on point clouds. Inverse Probl. Imaging **7**(3), 737–755 (2013)
Lai, R., Wen, Z., Yin, W., Gu, X., Lui, L.M.: Folding-free global conformal mapping for genus-0 surfaces by harmonic energy minimization. J. Sci. Comput. **58**(3), 705–725 (2014)
Lam, K.C., Lui, L.M.: Landmark-and intensity-based registration with large deformations via quasi-conformal maps. SIAM J. Imaging Sci. **7**(4), 2364–2392 (2014)
Lam, K.C., Gu, X., Lui, L.M.: Landmark constrained genus-one surface Teichmüller map applied to surface registration in medical imaging. Med. Image Anal. **25**(1), 45–55 (2015)
Lee, Y.T., Lam, K.C., Lui, L.M.: Landmark-matching transformation with large deformation via n-dimensional quasi-conformal maps. J. Sci. Comput. **67**(3), 926–954 (2016)
Lehto, O.: Quasiconformal Mappings in the Plane, vol. 126. Springer, Berlin/Heidelberg (1973)
Lei, N., Gu, X.: FFT-OT: a fast algorithm for optimal transportation. In: Proceedings of the IEEE/CVF International Conference on Computer Vision, pp. 6280–6289 (2021)
Lévy, B., Petitjean, S., Ray, N., Maillot, J.: Least squares conformal maps for automatic texture atlas generation. ACM Trans. Graph. **21**(3), 362–371 (2002)
Liang, J., Zhao, H.: Solving partial differential equations on point clouds. SIAM J. Sci. Comput. **35**(3), A1461–A1486 (2013)
Liang, J., Lai, R., Wong, T.W., Zhao, H.: Geometric understanding of point clouds using Laplace-Beltrami operator. In: Proceedings of the IEEE Conference on Computer Vision and Pattern Recognition, pp. 214–221 (2012)
Li, S., Zeng, W., Zhou, D., Gu, X., Gao, J.: Compact conformal map for greedy routing in wireless mobile sensor networks. IEEE Trans. Mobile Comput. **15**(7), 1632–1646 (2015)
Lipman, Y.: Bounded distortion mapping spaces for triangular meshes. ACM Trans. Graph. **31**(4), 1–13 (2012)

Lipman, Y., Kim, V.G., Funkhouser, T.A.: Simple formulas for quasiconformal plane deformations. ACM Trans. Graph. **31**(5), 1–13 (2012)
Liu, L., Ye, C., Ni, R., Fu, X.-M.: Progressive parameterizations. ACM Trans. Graph. **37**(4), 1–12 (2018)
Lui, L.M., Wen, C.: Geometric registration of high-genus surfaces. SIAM J. Imaging Sci. **7**(1), 337–365 (2014)
Lui, L.M., Wong, T.W., Thompson, P., Chan, T., Gu, X., Yau, S.-T.: Shape-based diffeomorphic registration on hippocampal surfaces using Beltrami holomorphic flow. In: International Conference on Medical Image Computing and Computer-Assisted Intervention, pp. 323–330. Springer, (2010)
Lui, L.M., Wong, T.W., Zeng, W., Gu, X., Thompson, P.M., Chan, T.F., Yau, S.-T.: Optimization of surface registrations using Beltrami holomorphic flow. J. Sci. Comput. **50**(3), 557–585 (2012)
Lui, L.M., Lam, K.C., Wong, T.W., Gu, X.: Texture map and video compression using Beltrami representation. SIAM J. Imaging Sci. **6**(4), 1880–1902 (2013)
Lui, L.M., Lam, K.C., Yau, S.-T., Gu, X.: Teichmüller mapping (T-map) and its applications to landmark matching registration. SIAM J. Imaging Sci. **7**(1), 391–426 (2014)
Lui, L.M., Gu, X., Yau, S.-T.: Convergence of an iterative algorithm for Teichmüller maps via harmonic energy optimization. Math. Comput. **84**(296), 2823–2842 (2015)
Meng, T., Lui, L.M.: PCBC: quasiconformality of point cloud mappings. J. Sci. Comput. **77**(1), 597–633 (2018)
Meng, Q., Li, B., Holstein, H., Liu, Y.: Parameterization of point-cloud freeform surfaces using adaptive sequential learning RBF networks. Pattern Recogn. **46**(8), 2361–2375 (2013)
Meng, T.W., Choi, G.P.-T., Lui, L.M.: TEMPO: feature-endowed Teichm̈uller extremal mappings of point clouds. SIAM J. Imaging Sci. **9**(4), 1922–1962 (2016)
Nadeem, S., Su, Z., Zeng, W., Kaufman, A., Gu, X.: Spherical parameterization balancing angle and area distortions. IEEE Trans. Vis. Comput. Graph. **23**(6), 1663–1676 (2016)
Ng, T.C., Gu, X., Lui, L.M.: Computing extremal Teichmüller map of multiply-connected domains via Beltrami holomorphic flow. J. Sci. Comput. **60**(2), 249–275 (2014)
Notomista, G., Saveriano, M.: Safety of dynamical systems with multiple non-convex unsafe sets using control barrier functions. IEEE Control Syst. Lett. **6**, 1136–1141 (2021)
Popov, D., Klimchik, A.: Real-time external contact force estimation and localization for collaborative robot. In: 2019 IEEE International Conference on Mechatronics, vol. 1, pp. 646–651. IEEE (2019)
Pumarola, A., Sanchez-Riera, J., Choi, G.P.T., Sanfeliu, A., Moreno-Noguer, F.: 3DPeople: modeling the geometry of dressed humans. In: Proceedings of the IEEE International Conference on Computer Vision, pp. 2242–2251 (2019)
Qiu, D., Lam, K.-C., Lui, L.-M.: Computing quasi-conformal folds. SIAM J. Imaging Sci. **12**(3), 1392–1424 (2019)
Rabinovich, M., Poranne, R., Panozzo, D., Sorkine-Hornung, O.: Scalable locally injective mappings. ACM Trans. Graph. **36**(4), 1 (2017)
Sawhney, R., Crane, K.: Boundary first flattening. ACM Trans. Graph. **37**(1), 1–14 (2017)
Shaqfa, M., Choi, G.P.T., Beyer, K.: Spherical cap harmonic analysis (SCHA) for characterising the morphology of rough surface patches. Powder Technol. **393**, 837–856 (2021)
Sharp, N., Crane, K.: A Laplacian for nonmanifold triangle meshes. Comput. Graph. Forum **39**(5), 69–80 (2020)
Sheffer, A., Praun, E., Rose, K.: Mesh parameterization methods and their applications. Found. Trends® Comput. Graph. Vis. **2**(2), 105–171 (2006)
Smith, J., Schaefer, S.: Bijective parameterization with free boundaries. ACM Trans. Graph. **34**(4), 1–9 (2015)
Su, K., Cui, L., Qian, K., Lei, N., Zhang, J., Zhang, M., Gu, X.D.: Area-preserving mesh parameterization for poly-annulus surfaces based on optimal mass transportation. Comput. Aided Geom. Des. **46**, 76–91 (2016)
Su, J.-P., Ye, C., Liu, L., Fu, X.-M.: Efficient bijective parameterizations. ACM Trans. Graph. **39**(4), 111–1 (2020)

Ta, D., Tu, Y., Lu, Z.-L., Wang, Y.: Quantitative characterization of the human retinotopic map based on quasiconformal mapping. Med. Image Anal. **75**, 102230 (2021)
Tewari, G., Gotsman, C., Gortler, S.J.: Meshing genus-1 point clouds using discrete one-forms. Comput. Graph. **30**(6), 917–926 (2006)
Tu, Y., Ta, D., Gu, X.D., Lu, Z.-L., Wang, Y.: Diffeomorphic registration for retinotopic mapping via quasiconformal mapping. In: 2020 IEEE 17th International Symposium on Biomedical Imaging, pp. 687–691. IEEE (2020)
Vogiatzis, P., Ma, M., Chen, S., Gu, X.D.: Computational design and additive manufacturing of periodic conformal metasurfaces by synthesizing topology optimization with conformal mapping. Comput. Methods Appl. Mech. Eng. **328**, 477–497 (2018)
Weber, O., Myles, A., Zorin, D.: Computing extremal quasiconformal maps. Comput. Graph. Forum **31**(5), 1679–1689 (2012)
Wen, C., Wang, D., Shi, L., Chu, W.C.W., Cheng, J.C.Y., Lui, L.M.: Landmark constrained registration of high-genus surfaces applied to vestibular system morphometry. Comput. Med. Imaging Graph. **44**, 1–12 (2015)
Wong, T.W., Zhao, H.-K.: Computation of quasi-conformal surface maps using discrete Beltrami flow. SIAM J. Imaging Sci. **7**(4), 2675–2699 (2014)
Wong, T.W., Zhao, H.-K.: Computing surface uniformization using discrete Beltrami flow. SIAM J. Sci. Comput. **37**(3), A1342–A1364 (2015)
Yang, Y.-J., Zeng, W.: Quasiconformal rectilinear map. Graph. Models **107**, 101057 (2020)
Yang, Y.-L., Guo, R., Luo, F., Hu, S.-M., Gu, X.: Generalized discrete Ricci flow. Comput. Graph. Forum **28**(7), 2005–2014 (2009)
Yin, X., Dai, J., Yau, S.-T., Gu, X.: Slit map: conformal parameterization for multiply connected surfaces. In: International Conference on Geometric Modeling and Processing, pp. 410–422. Springer (2008)
Yueh, M.-H., Lin, W.-W., Wu, C.-T., Yau, S.-T.: An efficient energy minimization for conformal parameterizations. J. Sci. Comput. **73**(1), 203–227 (2017)
Yueh, M.-H., Lin, W.-W., Wu, C.-T., Yau, S.-T.: A novel stretch energy minimization algorithm for equiareal parameterizations. J. Sci. Comput. **78**(3), 1353–1386 (2019)
Yueh, M.-H., Li, T., Lin, W.-W., Yau, S.-T.: A novel algorithm for volume-preserving parameterizations of 3-manifolds. SIAM J. Imaging Sci. **12**(2), 1071–1098 (2019)
Yueh, M.-H., Huang, H.-H., Li, T., Lin, W.-W., Yau, S.-T.: Optimized surface parameterizations with applications to chinese virtual broadcasting. Electron. Trans. Numer. Anal. **53**, 383–405 (2020)
Yung, C.P., Choi, G.P.T., Chen, K., Lui, L.M.: Efficient feature-based image registration by mapping sparsified surfaces. J. Vis. Commun. Image Represent. **55**, 561–571 (2018)
Zeng, W., Gu, X.D.: Registration for 3D surfaces with large deformations using quasi-conformal curvature flow. In: Proceedings of the 2011 IEEE Conference on Computer Vision and Pattern Recognition, pp. 2457–2464. IEEE (2011)
Zeng, W., Yang, Y.-J.: Colon flattening by landmark-driven optimal quasiconformal mapping. In: International Conference on Medical Image Computing and Computer-Assisted Intervention, pp. 244–251. Springer (2014)
Zeng, W., Yin, X., Zhang, M., Luo, F., Gu, X.: Generalized Koebe's method for conformal mapping multiply connected domains. In: 2009 SIAM/ACM Joint Conference on Geometric and Physical Modeling, pp. 89–100 (2009)
Zeng, W., Marino, J., Gurijala, K.C., Gu, X., Kaufman, A.: Supine and prone colon registration using quasi-conformal mapping. IEEE Trans. Vis. Comput. Graph. **16**(6), 1348–1357 (2010)
Zeng, W., Lui, L.M., Luo, F., Chan, T.F.-C., Yau, S.-T., Gu, D.X.: Computing quasiconformal maps using an auxiliary metric and discrete curvature flow. Numer. Math. **121**(4), 671–703 (2012)
Zhang, L., Liu, L., Gotsman, C., Huang, H.: Mesh reconstruction by meshless denoising and parameterization. Comput. Graph. **34**(3), 198–208 (2010)
Zhang, M., Guo, R., Zeng, W., Luo, F., Yau, S.-T., Gu, X.: The unified discrete surface Ricci flow. Graph. Models **76**(5), 321–339 (2014)

Zhang, M., Zeng, W., Guo, R., Luo, F., Gu, X.D.: Survey on discrete surface Ricci flow. J. Comput. Sci. Technol. **30**(3), 598–613 (2015)

Zhang, D., Choi, G.P.T., Zhang, J., Lui, L.M.: A unifying framework for n-dimensional quasi-conformal mappings. SIAM J. Imaging Sci. **15**(2), 960–988 (2022)

Zhao, X., Su, Z., Gu, X.D., Kaufman, A., Sun, J., Gao, J., Luo, F.: Area-preservation mapping using optimal mass transport. IEEE Trans. Vis. Comput. Graph. **19**(12), 2838–2847 (2013)

Zhao, J., Qi, X., Wen, C., Lei, N., Gu, X.: Automatic and robust skull registration based on discrete uniformization. In: Proceedings of the IEEE International Conference on Computer Vision, pp. 431–440 (2019)

Zhou, X.-Y., Ernst, S., Lee, S.-L.: Path planning for robot-enhanced cardiac radiofrequency catheter ablation. In: 2016 IEEE International Conference on Robotics and Automation, pp. 4172–4177. IEEE (2016)

Zou, G., Hu, J., Gu, X., Hua, J.: Authalic parameterization of general surfaces using Lie advection. IEEE Trans. Vis. Comput. Graph. **17**(12), 2005–2014 (2011)

Zwicker, M., Gotsman, C.: Meshing point clouds using spherical parameterization. In: Proceedings of the Eurographics Symposium on Point-Based Graphics, pp. 173–180 (2004)